AIAA JOURNAL
Vol. 41, No. 9, September 2003

Jet Aeroacoustic Testing: Issues and Implications

K. Viswanathan*
The Boeing Company, Seattle, Washington 98124-2207

Issues that are important for jet aeroacoustic tests and the critical role of good data in the development of jet noise technology are reviewed and discussed. A major effort for improving the quality of aeroacoustic data acquired at the Boeing Low Speed Aeroacoustic Facility has been carried out. This extensive undertaking targeted all aspects of model-scale testing and acquisition of good quality data and covered issues of flow quality, nozzle performance, and acoustics. Significant improvements have been made in all of the named categories. Simultaneous measurement of nozzle aerodynamic performance and noise is important, especially for the development of noise suppression devices. The capabilities of a jet rig incorporated with a six-component force balance are described. It is clearly demonstrated that the measured thrust with the current rig is in excellent agreement with that obtained using a dedicated force balance over a wide range of nozzle pressure ratios. Results of the efforts at rig refurbishment, carried out over the last few years, are presented. The high quality of noise measurements is established through good spectral agreement with data obtained with a blowdown jet, for a wide range of nozzle conditions. An extensive study of available jet noise data from various jet noise facilities has been completed. Implications of contaminated data from most tests and the obligations of the experimental community for the advancement of jet noise technology are discussed.

I. Introduction

JET noise is a major component of aircraft noise, especially during takeoff. The best way to minimize the impact of aircraft noise on communities close to airports is to reduce the noise at the source. As such, jet noise research that focuses on gaining a better understanding of the noise-generation mechanisms and the effects of realistic geometry and engine/airframe integration on the radiated noise is clearly warranted. Nearly five decades of research on jet noise has helped in our understanding of the fundamental mechanisms. However, to this day, no theory based on first principles that is capable of predicting the absolute spectral characteristics of the noise radiated to all angles by even a simple round nozzle exists. Most of the knowledge gained so far has been gleaned from jet noise measurements. All jet noise theories and methodologies based on these theories contain some level of empiricism, derived from measured data. Furthermore, all practical prediction methods for jet noise are empirical in nature; as such, they are only as good as the quality of the database on which they are based. Apart from the aforementioned needs of the theoretical community and practical prediction methods, there is the more pressing requirement of developing low-impact suppression devices for minimizing the acoustic signature of aircraft and mitigating community noise. Therefore, one cannot overstate the importance of acquiring good quality data and the critical role that data play in the development of noise reduction technology. Jet noise continues to be an area of active research for the stated reasons.

This paper deals mainly with the issues of data quality. One cannot consider the quality of noise data in isolation; the related issues of flow quality and aerodynamic performance of the nozzle must also be kept in mind, to ensure that the measured data are meaningful. Several experimental studies have been carried out in the last few years by the aerospace industry, as well as NASA, as part of the Advanced Subsonic Transport program. These studies focused on achieving jet noise reduction through suitable modifications to the nozzle trailing edge, through the incorporation of tabs, chevrons, vortex generators, etc. To evaluate these devices, it is of paramount importance to minimize rig or extraneous noise so that the true effect of these devices may be uncovered. One must also quantify carefully the impact of these devices on thrust, apart from their potential for noise reduction. The thrust degradation caused by past noise suppression devices has rendered most of them unsuitable for airplane application. Usually, two separate tests are conducted, one for noise and one for thrust. However, it is preferable to measure both the noise and performance simultaneously, to eliminate the variabilities and uncertainties caused by the different upstream conditions prevailing in the two facilities. The importance of assessing both the noise and thrust simultaneously was well recognized in the High Speed Research/High Speed Civil Transport (HSR) program, where a takeoff noise reduction of ~20 dB in effective perceived noise level (EPNL) was required to meet the noise goals. It can be readily appreciated that a significant performance penalty would be incurred by any concept that could potentially provide such a large reduction in noise and that it was vital to quantify the thrust degradation.

To meet the test requirements of the HSR program, a jet simulator was designed and built by The Boeing Company in the early 1990s, referred to as the NTL3800 rig. The jet rig consists of high-temperature supply piping, burners, instrumentation, and aerodynamic fairings designed for a high flow capability of 20 lb/s (9.07 kg/s) in single-flow mode and 30 lb/s (13.61 kg/s) in dual-flow mode, for continuous operation. Both of the streams may be heated to 1950°R (1083 K) to simulate inverted-velocity-profile jets, if desired. This jet rig is integrated with a six-component force balance, referred to as the E-3 balance. This rig was used exclusively by the HSR program, and hence, none of the test results or the capabilities of the rig published in the open literature. Initial checkout and validation tests of this rig, with simple round nozzles, were carried out once the rig was operational. However, the author noted several anomalous trends in the measured spectra. There was also a high level of flow distortion. An extensive refurbishment of the rig was carried out in 1998, before an HSR nozzle development test. Numerous modifications were incorporated, and the extraneous rig noise substantially reduced. The results of this effort were reported to the HSR aeroacoustic community. However, it was realized at that time that additional improvements were necessary.

More recently, another major effort for improving the quality of aeroacoustic data acquired at the Boeing Low Speed Aeroacoustic Facility (LSAF) has been carried out by the author. This undertaking

Received 5 November 2001; presented as Paper 2002-0365 at the AIAA 40th Aerospace Sciences Meeting, Reno, NV, 14–17 January 2002; revision received 25 February 2003; accepted for publication 9 April 2003.

*Engineer, Aeroacoustics and Fluid Mechanics, Mail Stop 67-ML, P.O. Box 3707; k.viswanathan@boeing.com. Senior Member AIAA.

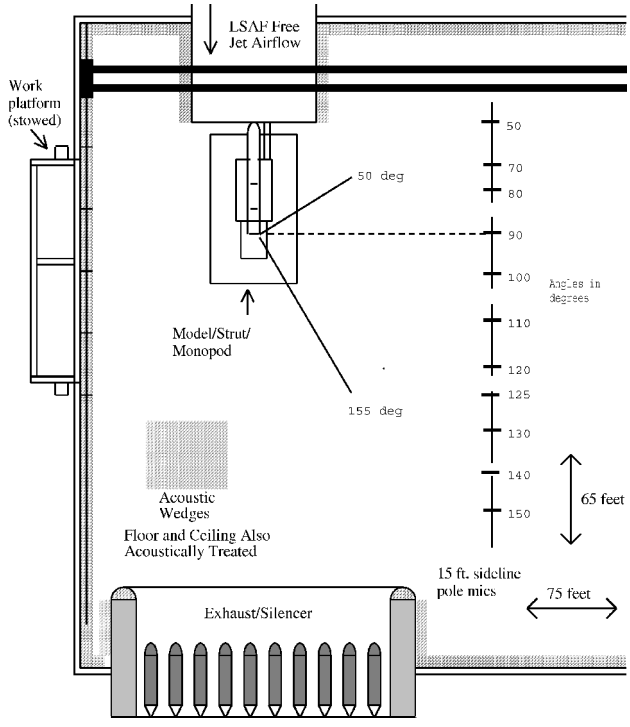

Fig. 1a Plan view of LSAF test cell (not to scale).

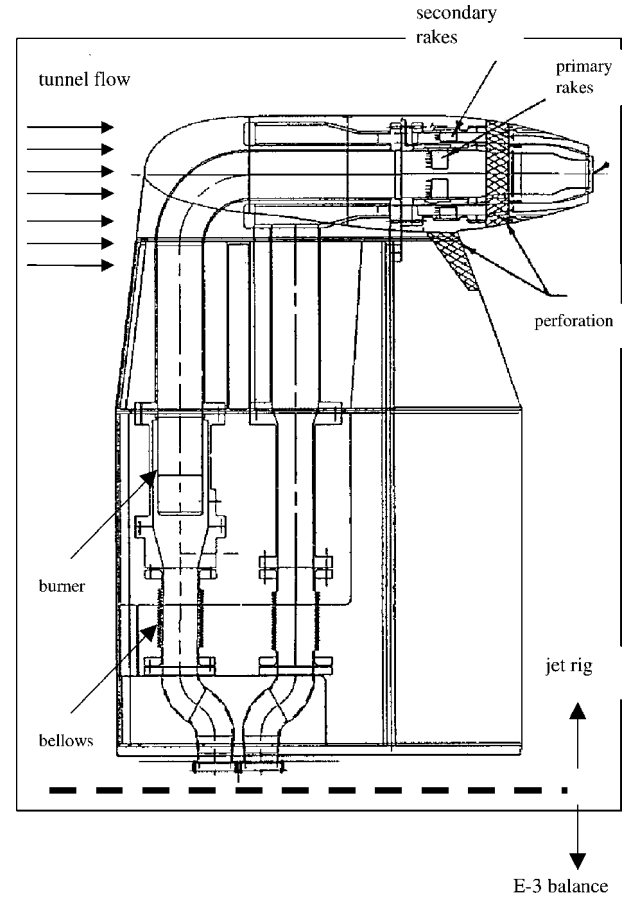

Fig. 1b Schematic of NTL3800 jet simulator.

targeted all aspects of model-scale testing and acquisition of good-quality data and covered issues of flow quality, nozzle performance, and acoustics. Significant improvements have been made in all of the categories. Salient results from the work carried out in stages over several years are reported here.

An extensive analysis of available jet noise data from various jet noise facilities has also been carried out. It is shown that most data suffer from contamination from nonjet sources. The implications of these data in the development of noise-reduction devices are examined and explained with examples of actual measured data. Finally, it is stressed that rig noise issues be addressed by the experimental community followed by a few recommendations for future tests.

II. Description of the Jet Simulator

Brief descriptions of the test cell and the features of the NTL3800 jet rig are first given. A schematic of the plan view of the test cell is shown in Fig. 1a and that of the jet simulator and support in Fig. 1b. Figure 1a shows the placement of the jet rig, the wind tunnel, and the layout for the microphones. The microphones are mounted on poles and are at the same height as the centerline of the jet, about 17.2 ft (5.3 m) above the ground. As already stated, the rig has a high enough mass flow capability to meet the requirements of most scale-model tests. The rig also has provision to control the external boundary-layer growth. A vacuum system with two perforated sections is located upstream of the model. When the suction through the perforated skin is controlled, the thickness of the external boundary layer may be controlled.

The six-component balance can pass two airflow lines, fuel flow lines, and a vacuum line for the control of the boundary layer, across the balance plane. The support structure for the balance and a service module (which routes instrumentation and control cables and fuel and hydraulic lines) are mounted on air bearings and may be placed anywhere within the anechoic chamber. All air lines, fuel lines, and instrumentation are contained within an aerodynamic strut. This strut has provisions for all of the lines to be passed across the balance interface in a manner that avoids interference with force measurements.

III. Issues with Data Quality

The major achievements in improved flow quality and in the reduction of rig noise are now presented. Concrete examples are shown to illustrate the different aspects. The importance of the upstream plenum and size of the supply pipe in reducing the internally generated rig noise is well known. In past acoustic tests,[1–4] very large contraction ratios (plenum cross-sectional area/nozzle throat area) were employed to minimize upstream disturbances. This arrangement is good for acquiring static noise data. However, a compact rig is needed when the effects of forward flight need to be evaluated, by embedding the rig in wind-tunnel flow. The size of the rig is then dictated by considerations of the size of the wind-tunnel, wind-tunnel blockage effects, boattail angle, etc. This requirement of a compact rig necessarily introduces several problems as will be discussed.

A. Flow Quality

The primary and secondary supply lines for the NTL3800 consist of 8-in.-diam pipes, to meet the flow requirements and yet keep the size of the aerodynamic strut reasonably small. The size of the nozzle tested then determines the contraction ratio. The jet simulator has a close-coupled propane burner, which is inside the strut as shown in Fig. 1b. The burner consists of a fuel injector and a swirl plate upstream to enhance mixing of the fuel with air. Only a portion of the incoming air goes through the burner; the rest of the flow bypasses the burner (thereby providing a cooling flow on the outside) and is injected downstream of the combustion zone. The cold and hot streams mix downstream, before they reach the nozzle entrance section. As can be seen in Fig. 1b, there is no room to accommodate a plenum downstream of the burner and there is only a short distance with a 90-deg bend, before the flow reaches the charging station. Flow characteristics at the nozzle entrance are measured using pressure and temperature rakes installed in the charging station. Figure 2 shows a schematic of the rake system. There are three temperature and three pressure rakes, in the two streams. There are five transducers, located on centroids of equal area, in each primary rake. In the secondary flow, the pressure rakes again have five transducers, whereas the temperature rakes have three.

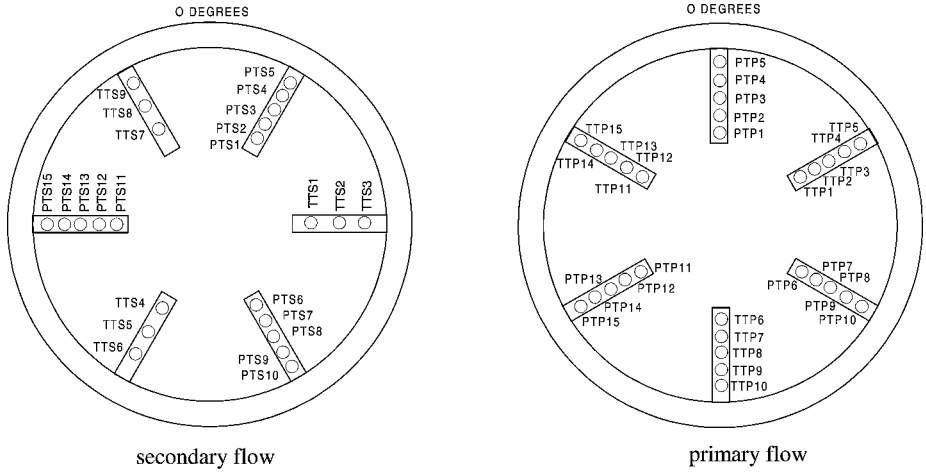

Fig. 2 Flow measurement system.

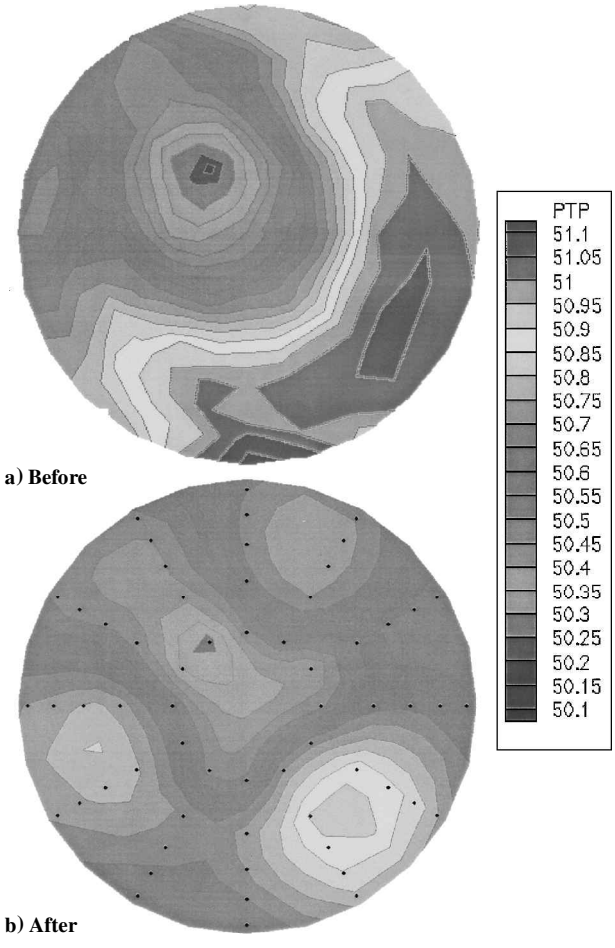

Fig. 3 Pressure distribution before and after improvements.

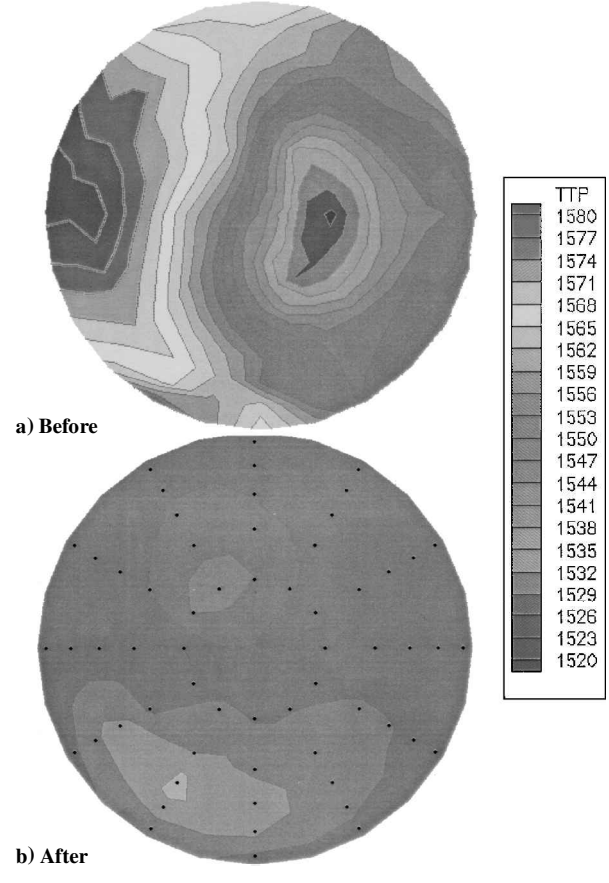

Fig. 4 Temperature distribution before and after improvements.

The nozzle conditions are established by averaging the readings of the 15 probes for pressures and 15 and 9 thermocouples in the primary and secondary streams, respectively. The goodness of the flow is monitored through the calculation of distortion factors, defined as $[(\phi_{\max} - \phi_{\min})/\phi_{\text{av}}]$, where ϕ is either reservoir pressure or temperature. In the early attempts at improving the aeroacoustic quality, which consisted of installing flow conditioners and blockage devices, it was found that one could improve the flow quality or noise, but not both simultaneously. After many design improvements and modifications to the entire flow system and the fuel system, acceptable results were obtained. Figure 3 shows a contour plot of the measured pressures before and after the improvements. In Fig. 3a, one may identify a large region of high pressure (red) and a region of low pressure close to the center of the duct. In the Fig. 3b, a more uniform pressure prevails in the entire cross-sectional area. Figure 4 shows a similar plot for the temperature distribution. The data were acquired thrice, with the rakes rotated clockwise by 30 deg each time, to map out the entire flowfield. Again, the temperature distribution is uniform. Quantitative measures of the distortions in pressure and temperature are shown in Figs. 5 and 6, respectively, for a wide range of nozzle pressure ratio (NPR) and reservoir temperature. As can be seen, the distortion level is extremely low, less than 1% for all of the cases. The typical temperature at takeoff power for an engine is $\sim$1500°R. It is clear from Fig. 6 that the rake-to-rake variation in total temperature is $\sim \pm 5$°R. To put this value in context,

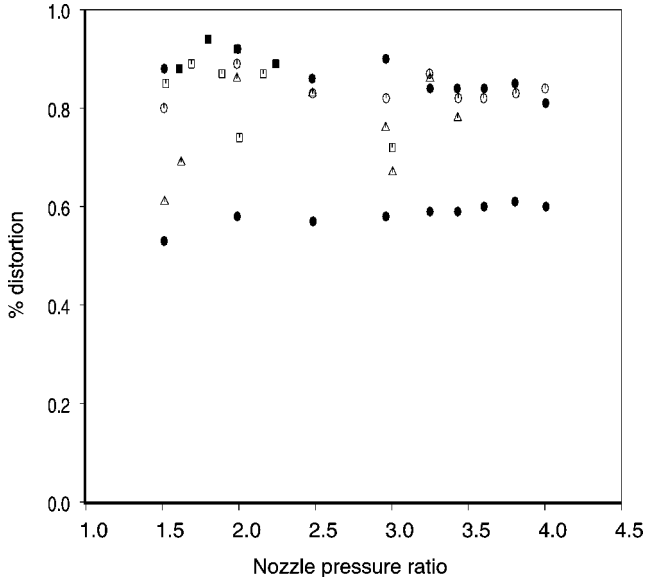

Fig. 5 Variation of pressure distortion with NPR: symbols, different cycle conditions.

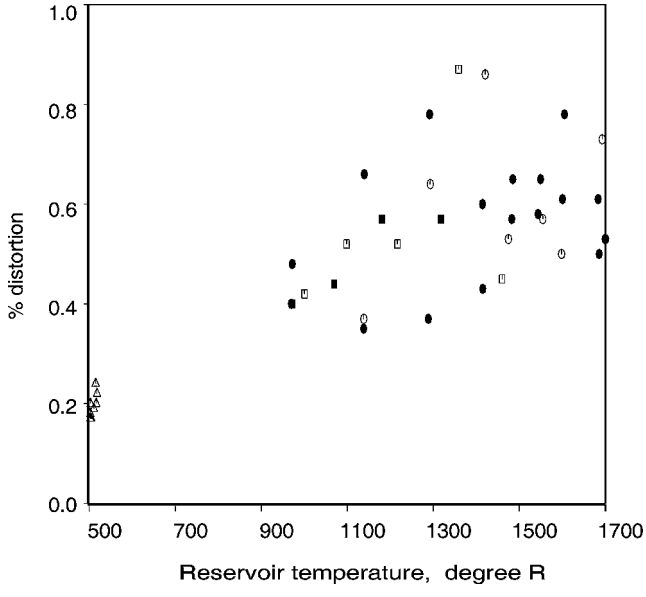

Fig. 6 Variation of temperature distortion with reservoir temperature: symbols, different cycle conditions.

note that rake-to-rake variations of several hundred degrees have been observed in some past tests. These data were acquired with a standard nozzle, as defined by the American Society of Mechanical Engineers, with a diameter of 4.93 in. However, one may not achieve this degree of uniformity under all conditions. When smaller nozzles are used, with correspondingly lower mass flow rates, the temperature distortions tend to be higher.

B. Nozzle Aerodynamic Performance

The gasdynamic equations for the flow in a nozzle are well known and are not reproduced here. The plenum pressure and temperature at the nozzle entrance are given by the rake averages. One may calculate the ideal velocity from these values and the ideal mass flow rate, for a given nozzle size. Critical flow venturis installed in the primary and secondary supply ducts provide the actual mass flow rates. One may define the characteristics of the nozzle aerodynamic performance, discharge, and thrust coefficients, as follows:

$$C_d = W_{\text{actual}} / W_{\text{ideal}}, \qquad C_f = F_{\text{measured}} / (W_{\text{actual}} \times V_{\text{ideal}})$$

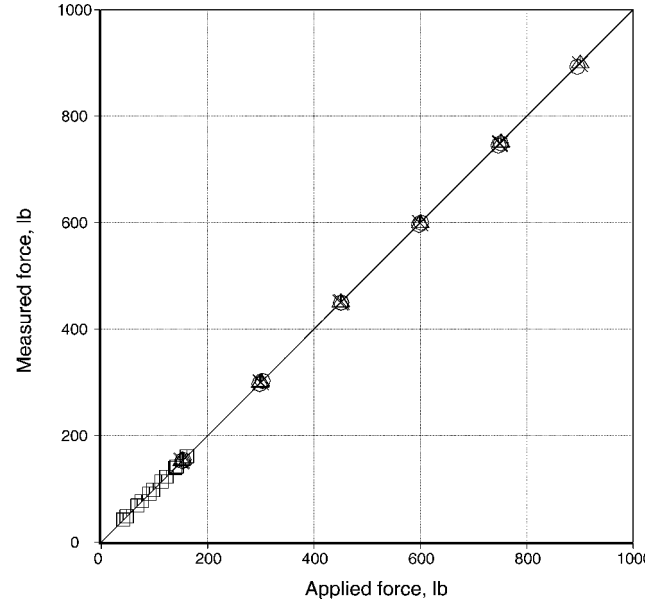

Fig. 7 Response of the balance to applied load: symbols, different repeats and ——, ideal response.

The axial force measured by the balance is used in the evaluation of the thrust coefficient.

In the past tests with single-stream nozzles, the secondary supply line was used to remove the boundary-layer bleed through the aerodynamic strut. To test dual-stream nozzles and still permit the use of the bleed system, an additional evacuation line was added. The force balance was recalibrated, and the response of the balance to applied individual loads and moments; combinations of loads and moments; and individual primary, secondary, and vacuum pressure tares, and combinations thereof was measured. A coefficient matrix of residuals generated from this large database of measured tares is then used to interpret the balance readings when a nozzle test is conducted.

For a nozzle test, the primary force component of interest is the axial force or thrust. To ensure that there is no drift in the balance readings during the course of a long test, the fidelity of the measured axial force component is checked periodically. Figure 7 shows the response of the balance for a known applied load; the symbols denote the results from different checks and the straight line the ideal response (a straight line with a slope of 45 deg). As can be seen, the repeatability and accuracy are very good. Now we show sample results of the aerodynamic performance of the nozzle. Figure 8 shows the variation of the thrust coefficient with NPR, for a 4-in.-cubic nozzle. There are two sets of data: one obtained with the E-3 balance and another one with the Boeing Nozzle Test Facility (NTF) balance. The NTF is a dedicated facility for measuring nozzle performance, is well established, and has been used widely by the industry for over two decades. There is excellent agreement between the two sets of data over the entire range of pressure ratios.

The preceding set of results was obtained with the primary airstream. For simulations of turbofan engines, measurements from coaxial nozzles are necessary. To check the quality of the secondary flow system independently, the same measurements were repeated with the same cubic nozzle. However, the nozzle was supplied with secondary air, as illustrated by the layouts of the nozzle arrangements for the earlier two situations in Figs. 9a and 9b. Note that the upstream flowpaths are very different, as seen in Fig. 1b: The secondary stream empties into a plenum of larger cross-sectional area, followed by a contraction. The variations of the nozzle discharge and thrust coefficients with NPR for the two arrangements are shown in Figs. 10 and 11, respectively. There is excellent agreement between the discharge coefficients obtained with the different supply streams. This is, of course, expected. However, there is a difference in the thrust coefficients, with the values obtained with the

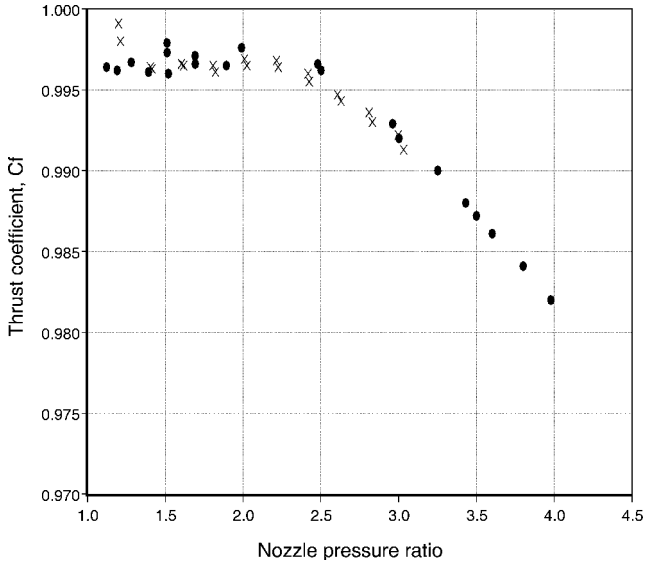

Fig. 8 Variation of thrust coefficient with NPR: ×, NTF balance and ●, E-3 balance.

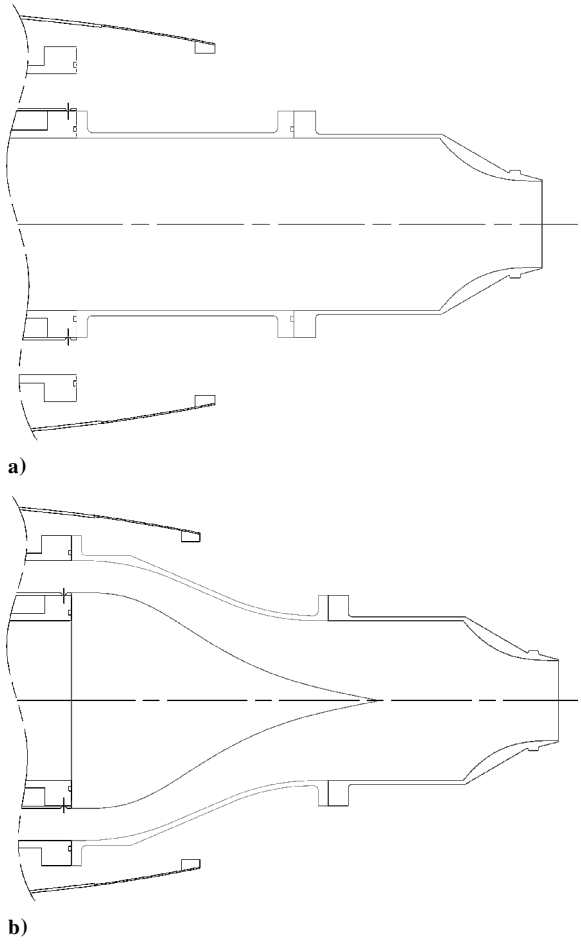

Fig. 9 Layout of the nozzle arrangements: a) primary air supply and b) secondary air supply.

secondary supply lower by ~0.2%. This consistent shift, over the entire range of NPR, rules out the possibility of scatter and points to a potential error in the tare estimate. This is the first time that the supply systems were independently evaluated. It has been estimated from the current and past tests that the error of the entire system is less than ±0.2%. This level of accuracy is extremely good. Consistency and repeatability of performance data are demonstrated as part of the discussions in the next section.

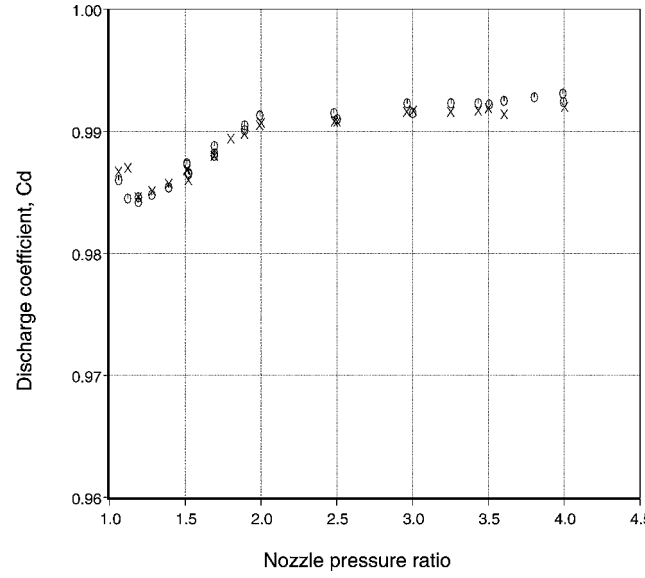

Fig. 10 Variation of discharge coefficient with NPR: ×, primary air supply and ○, secondary air supply.

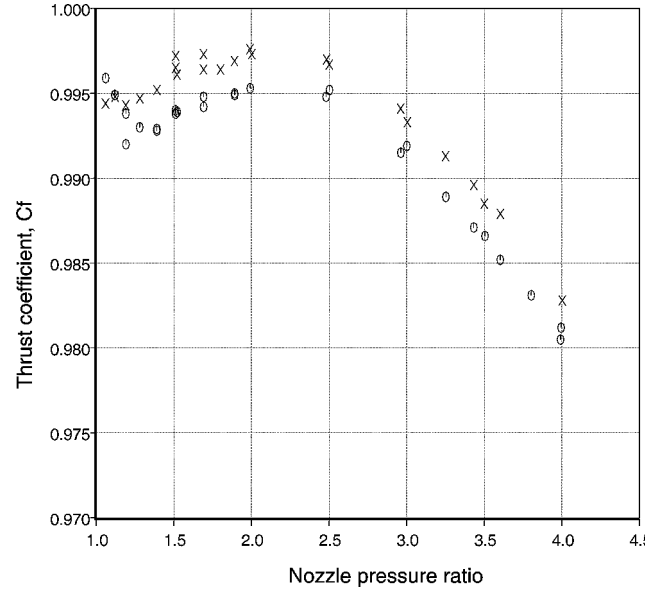

Fig. 11 Variation of thrust coefficient with NPR: ×, primary air supply and ○, secondary air supply.

C. Acoustics

As stated earlier, the jet simulator is embedded in a wind tunnel (Fig. 1a), which can provide a maximum freestream Mach number of 0.32. The microphones are laid out at a constant sideline distance of 15 ft (4.572 m) from the jet axis, except the microphone at 155 deg, which is at a distance of 12.75 ft (3.886 m). Thus, the slant distance to the microphone is a minimum at 90 deg and keeps increasing as the angle becomes more oblique. All angles are measured from the jet inlet axis, with a polar angular range of 50–155 deg. Additional microphones are also located at several polar angles at a different azimuthal angle. Bruel and Kjaer Type 4939 microphones (newer type that replaced Type 4135) are used for free-field measurements. The microphones are set at normal incidence and without the protective grid, which yields a flat frequency response up to 100 kHz. Narrowband data with a bandwidth of 23.4 Hz are acquired and synthesized to produce one-third-octave spectra, up to a center band frequency of 80,000 Hz.

The reduction/elimination of rig noise presents a formidable challenge because the sources of noise are myriad. Whereas one could improve the flow quality by installing mixing enhancement devices

and screens, strategies for reducing rig noise are not very obvious. Noise from valves, pumps, and combustors, flow noise due to high flow velocities in the ducts and sharp bends, and several other internal noise sources such as due to flow over steps, gaps, screw heads, etc., have rendered much of the data hopelessly contaminated. Many anomalous trends have been noted in the past experiments, due to a variety of problems with the test facilities and instrumentation. It is important to understand and minimize the deleterious effect of the rig noise, especially at low jet velocities. If the situation is bad for static noise measurements, it only gets worse for wind-on testing. Now, one has to contend with the tunnel noise level, noise generated by the collector, hydraulic systems, etc., in addition to the rig noise.

1. *Qualitative Evaluations*

How then to ensure that the measured noise is free of contamination? Qualitative checks may be performed easily now. A few years ago, Tam et al.[5] showed conclusively that the jet noise spectrum from single-stream nozzles at low inlet angles (in the forward quadrant and in the near-normal angles) conform to a universal shape. More recently, Viswanathan[6] offered proof that the shapes of the spectra from coaxial nozzles also have the same similarity shape irrespective of jet operating conditions such as pressures, temperatures, area ratio, velocity ratio, bypass ratio, etc., of the two streams. The significance of an important effect, due to atmospheric attenuation, was also discussed in depth in Ref. 6. It was pointed out that there is no easy fix for the omission of this effect, and it was recommended that the shape of the universal spectrum at the higher frequencies be redetermined from data normalized to standard conditions. However, the universal shape as determined by Tam et al.[5] are employed in the following sections, while fully recognizing the effect of atmospheric attenuation on spectral shapes at the higher frequencies. Let us examine the spectral shape now. Figure 12 shows a comparison of the measured spectra and the fine-scale similarity spectrum (FSS) at 90 deg, from unheated jets at several Mach numbers of 0.3, 0.4, 0.5, 0.6, 0.7, 0.8, 0.9, and 1.0. There is excellent agreement for Mach numbers 0.6 and higher. However, at a Mach number of 0.5, the data at the highest frequencies are slightly higher than the empirical curve. At $M = 0.4$, the discrepancy is more pronounced, and the spectrum starts deviating above a frequency of 20,000 Hz [band 43, where band number $= 10 \times \log(f)$, and f is frequency in hertz]. The spectrum at $M = 0.3$ does not resemble that of jet noise at all and is corrupted completely by rig noise.

One could measure the rig noise for a given reservoir temperature by using two nozzles of different sizes. The NPR that corresponds to a desired Mach number is set with the smaller nozzle, and the mass flow rate for this nozzle is calculated. The NPR for the larger nozzle is determined to provide the same mass flow rate obtained with the smaller nozzle. Because the mass flow in the supply pipe is the same, the internal noise is the same for the two cases. However, the jet velocities are different, and one could estimate the intensities of the radiated noise using the V^8 law. It may be shown easily, when scaled to unit area, that the ratio of intensities is given by

$$I_1/I_2 \approx (d_2/d_1)^{16}$$

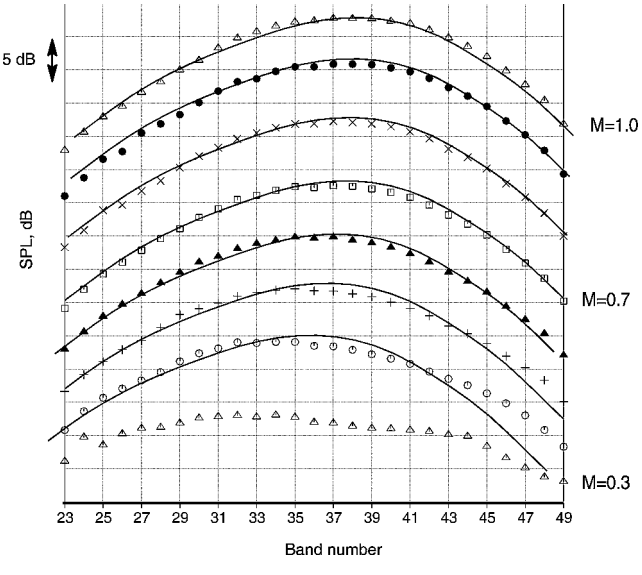

Fig. 12 Comparison of spectra from cold jets, D = 1.5 in., angle = 90 deg: △, M = 0.3; ○, M = 0.4; +, M = 0.5; ▲, M = 0.6; □, M = 0.7; ×, M = 0.8; ●, M = 0.9; ⚠, M = 1.0; and ——, FSS spectrum.

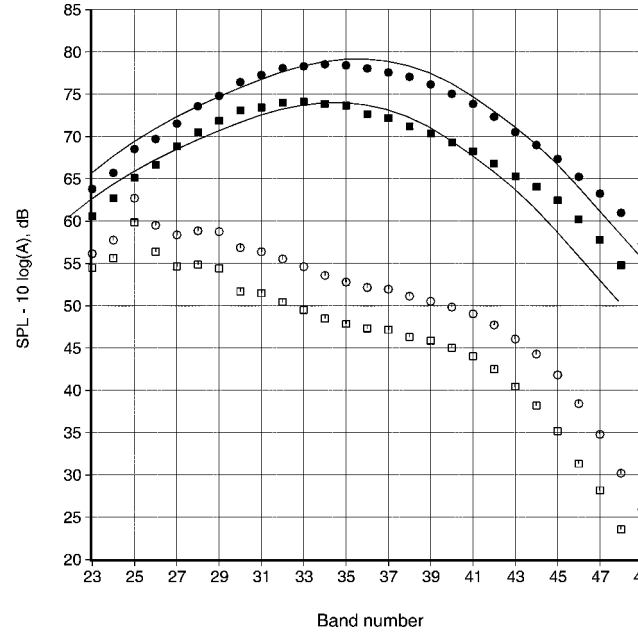

Fig. 13 Estimation of rig noise at 90 deg, T_r/T_a = 3.2: ■, M = 0.4 and d = 2.45 in.; ●, M = 0.5 and d = 2.45 in.; □, M = 0.4 and d = 4 in.; ○, M = 0.5 and d = 4 in.; and ——, FSS spectrum.

In Fig. 13, we show the results of this exercise for two Mach numbers of 0.4 and 0.5 and at a temperature ratio $T_r/T_a = 3.2$. The noise levels have been adjusted by subtracting $[10 \times \log(A)]$ to yield noise per unit area. The dark symbols represent the spectra from the smaller nozzle ($d = 2.45$ in.), whereas the corresponding open symbols represent the spectra from a larger nozzle ($d = 4.0$ in.). The preceding expression yields a difference of ~34 dB in the noise levels; although approximate, it still is a very large number. Let us examine the spectra at 90 deg. The noise level of the larger nozzle is definitely not what it should be, and hence, the spectra represent the rig noise at these conditions. Because most of the noise is internally generated, it is not clear as to what diameter should be used for scaling the frequency. Therefore, the 2^+ one-third-octave band shift was not applied in Fig. 13. However, this does not change the message. Usually, it is argued that because the noise level of the smaller nozzle is well above the rig noise, except for the lowest frequencies in Fig. 13, the data are of good quality. However, this is not true as indicated by comparisons with the similarity spectrum. There is a small discrepancy of ~2 dB at the higher frequencies for the $M = 0.5$ jet. For the lower-Mach-number case, the levels are off by ~5 dB above 20,000 Hz.

This method of trying to measure rig noise just indicates that the noise from the larger nozzle is not correct. However, it does not guarantee that the noise from the smaller nozzle is good. In fact, the spectra do look good at first blush. However as already shown, appearances can be deceiving. Experience has shown that simple round nozzles produce spectra that conform to a universal shape at lower inlet angles. As illustrated with the preceding examples, we have utilized this knowledge and demonstrated a reliable way to check spectral shapes. One could adopt this approach with narrowband data as well. However, in the author's opinion, it is preferable to use one-third-octave band data for the following reason. Good narrowband data tend to have wiggles of ~1–2 dB. When the anechoicity

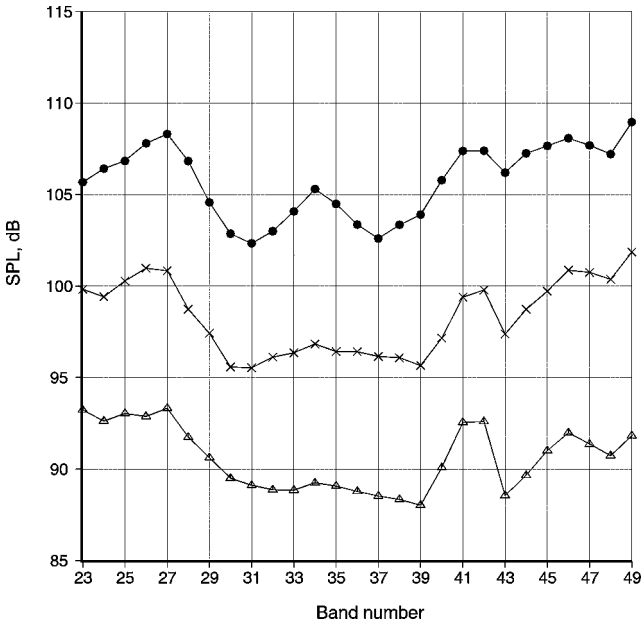

Fig. 14 Typical spectra before improvements at lower angles and two power settings.

of the chamber is not good or perhaps due to reflections and other rig problems, larger wiggles of ~3–5 dB have been observed. This ringing in the data could potentially provide a better fit with the similarity spectrum than is warranted, thereby masking imperfections in the data.

2. Rig Modifications and Improvements

Now we present the results of the many modifications to the rig and the resultant improvements in data quality. Figure 14 shows typical initially measured spectra at lower angles from heated jets at two power settings. It is obvious that the spectra are hopelessly contaminated by extraneous noise, with the low- and high-frequency portions tailing up instead of down. The spectra at other angles were also contaminated, with a tail-up at the higher frequencies. It was reasoned that the discrepancy must be due to several problems because a single noise source from the rig was unlikely to affect all of the frequencies, especially to this extent. This reasoning led to a critical evaluation of the entire flow system and the jet rig, electronics, microphone setting, data acquisition system, etc. Needless to say, many problems were uncovered with every component, and suitable modifications were devised as necessary. First, problems with the measurement system such as the dynamic range, high electronics noise floor, etc., were identified and fixed. Then came rig modifications that included the redesign and the elimination of a few 90-deg bends in the supply pipe, installation of a screen upstream of the burner, redesign of the fuel pump and the fuel nozzle, design and installation of choke plates downstream of the burner for improving mixing and reducing combustor noise, installation inside the primary supply pipe of a smaller diameter pipe with paddles that introduce axial vorticity and promote mixing, and many others. These were the modifications alluded to in Sec. III.A, where the improvement in flow quality was presented. Figure 15 shows the corresponding improvement in noise data from a heated jet at high subsonic Mach number, with comparison of spectra before and after the incorporation of numerous changes. The spectra at three angles of 60, 110, and 145 deg, which cover a wide range of radiation angles, are shown. A noise reduction of more than 10 dB, over a wide range of frequencies (from 200 to ~5000 Hz), at all angles is seen. Although it was known that there were problems with the data, the magnitude of the contamination was not fully understood. The improved spectra at the two lower angles shown are smooth and at least resemble that of jet noise, with the behavior at low frequency as per expectation. Comparison with the spectral shapes shown in Fig. 14 illustrates dramatically the progress made

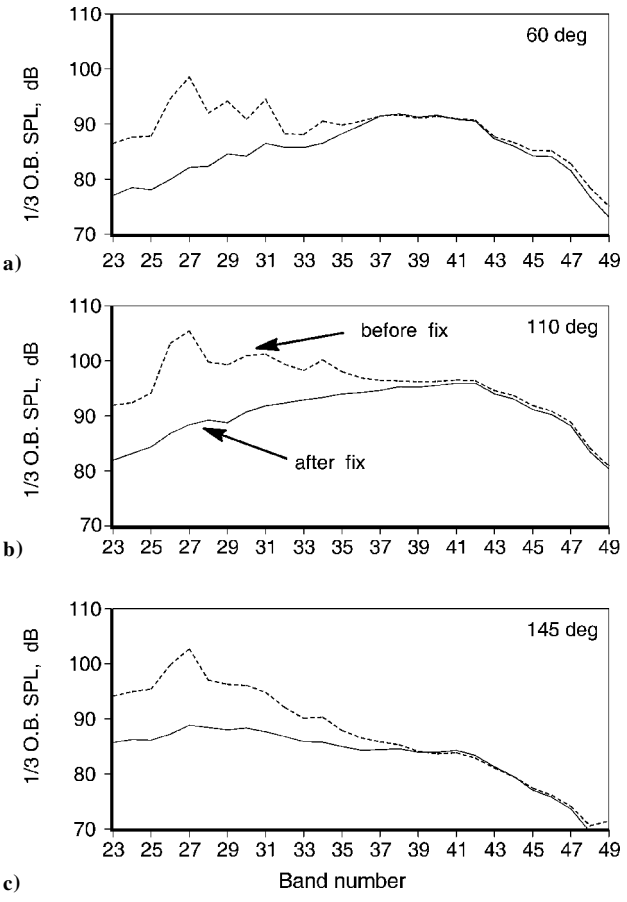

Fig. 15 Rig noise reduction and improvements in acoustic data.

in reducing extraneous noise and acquiring good-quality data. The demonstrated reduction in rig noise over a wide range of frequencies and at all angles has highlighted the severity and extent of the problem. This exercise should serve as a cautionary tale for future tests.

Before we examine the quantitative goodness of the spectra, another feature of the jet rig is described. In an earlier section, it was mentioned that the external boundary layer on the nozzle might be controlled by means of a vacuum system. It is important to maintain the proper boundary-layer thickness for two reasons. In an engine installation, the ratio of the nacelle length to engine diameter is $\sim\vartheta(1)$. However, in the jet simulator, as seen in Fig. 1, this ratio has a very large value. Consequently, the boundary layer builds up over a much longer distance over the strut. To obtain the true forward-flight effects, the boundary-layer thickness in the jet simulator must be reduced to preserve geometric similarity between the scale model test and an engine test. The second reason, the more important one, for controlling the boundary-layer thickness pertains to scale model tests of mixer-ejector nozzles. When the noise reduction potential of ejectors is evaluated, it is imperative to provide a clean flow of the entrained air into the ejector. This vital requirement forced us to examine the vacuum system in detail. In past tests, it was not realized that the vacuum system produced a tremendous amount of high-frequency noise, which contaminated the spectra during wind-on testing. Let us now examine the effect of the boundary-layer control system on flow and noise. Figure 16 shows the boundary-layer profiles for various rates of suction, obtained with a rake containing 14 probes. To establish the baseline values of the noise and the condition of the boundary layer, a solid fairing was designed and installed over the perforated sections first. The profile corresponding to this configuration, denoted by the dotted line and labeled hardwall-no bleed in Fig. 16, has a thick boundary layer. As we gradually increase the suction rate, the profile becomes fuller and the boundary layer thinner as shown. Note that there is only negligible effect when the

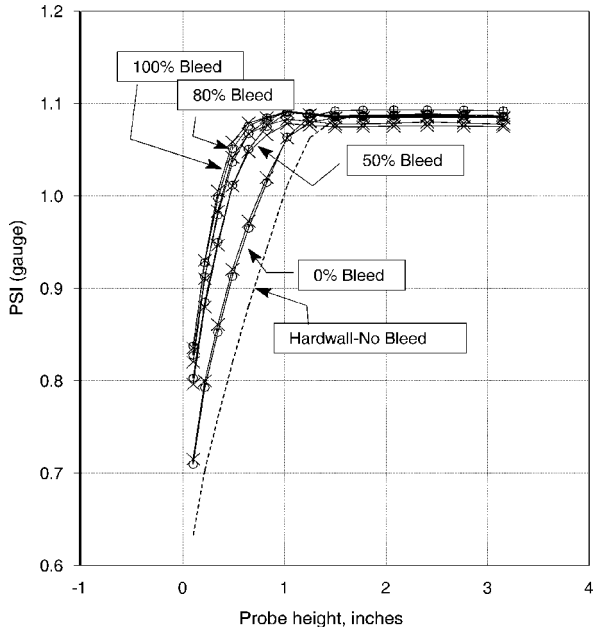

Fig. 16 Variation of the boundary-layer profile with suction, $M_t = 0.32$.

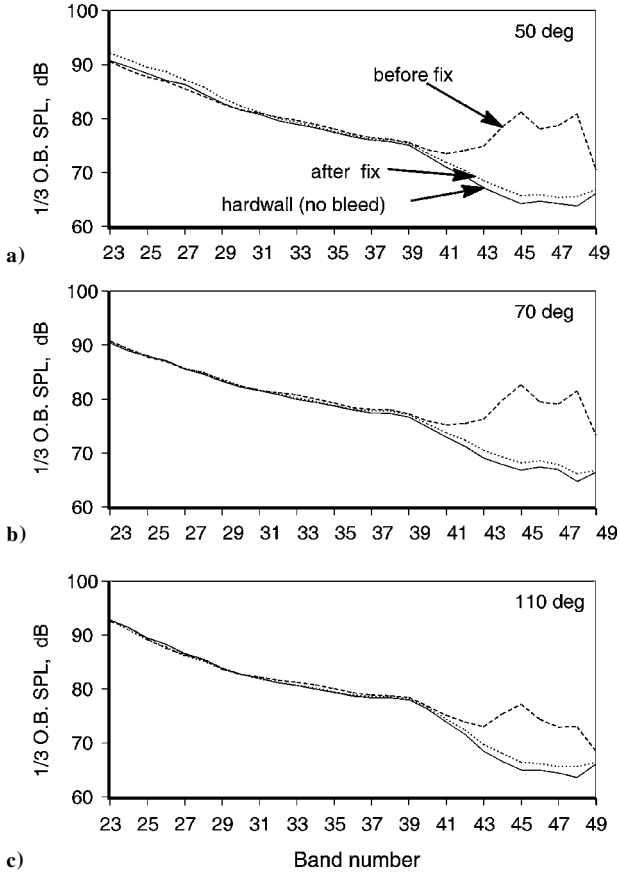

Fig. 17 Reduction of background noise due to wind tunnel and vacuum system, $M_t = 0.32$.

bleed rate is increased from 80 to 100%, where the bleed percentage is set by the revolutions per minute of the motor.

The noise floor set by the vacuum system (not shown here) alone was found to be low. Figure 17 shows the background noise at three angles when the tunnel is operated at a Mach number of 0.32. Three curves are shown in each of Figs. 17a–17c. The solid line corresponds to that from the baseline, with the perforations completely covered; this line represents the minimum noise. As the vacuum

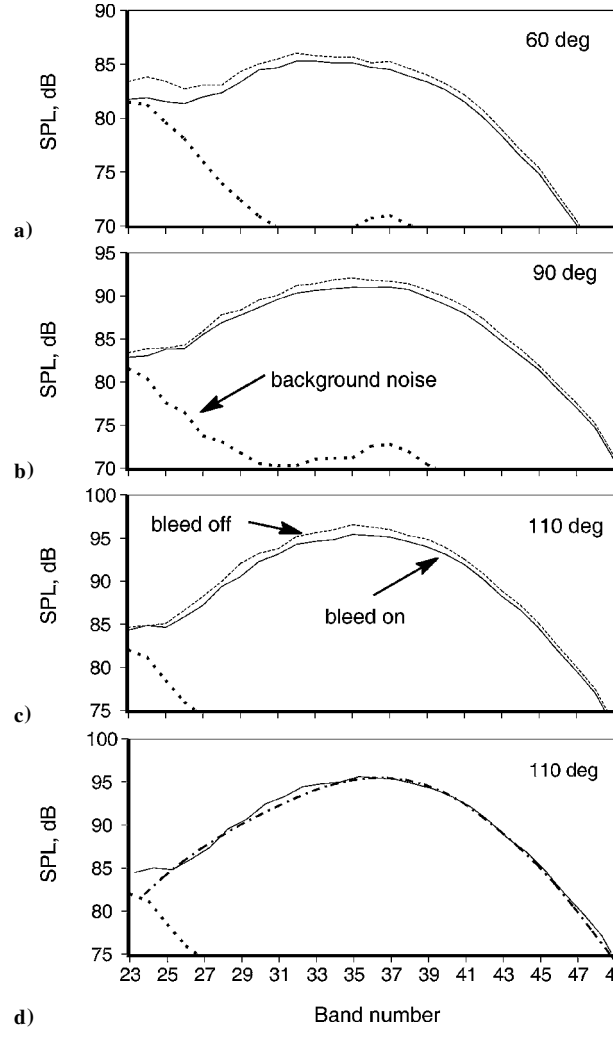

Fig. 18 Effect of external boundary-layer thickness on radiated noise; $M_j = 0.8$, $T_r/T_a = 2.7$, $M_t = 0.24$: - - - -, bleed off; ——, bleed on; · · ·, background noise; and –·–·, FSS.

motor is turned on with the tunnel running, the lower momentum air is bled off, thereby bringing the high-speed air closer to the perforations. The resultant scrubbing of high-velocity flow on the perforations generates a tremendous amount of high-frequency noise, nearly ~15 dB for frequencies above 10,000 Hz (see the dashed lines in Figs. 17). This noise increase was found to be a direct function of the bleed rate (the curve shown is for a bleed rate of 80%). To fix this problem, a screen fabricated with a very fine mesh was installed over the perforations. The background noise from this configuration is denoted by the dotted lines in Figs. 17. It is clear that this fix has eliminated the generation of the high-frequency noise. Based on the noise and boundary-layer measurements, it was decided to run the vacuum system at a bleed rate of 80% when evaluating forward flight effects. In Fig. 18, we show the effect of reducing the boundary-layer thickness on the far-field noise. Recently measured spectra at three low radiation angles, with and without the bleed, are shown in Fig. 18. The jet Mach number was 0.8, the temperature ratio was 2.7, and the tunnel Mach number was 0.24. Also shown in Fig. 18 is the background noise, denoted by the dotted lines. When the bleed system is operated, we observe a reduction of 1–2 dB across the entire spectrum at the lower angles. There is only a negligible effect at high aft angles. This reduction is dependent on the nozzle size and geometry, jet operating conditions, etc. In Fig. 18d, we show a comparison with the FSS spectrum. It is evident that the measured spectrum is in good agreement with the FSS, confirming that the universal shape is maintained when there is an external airstream.

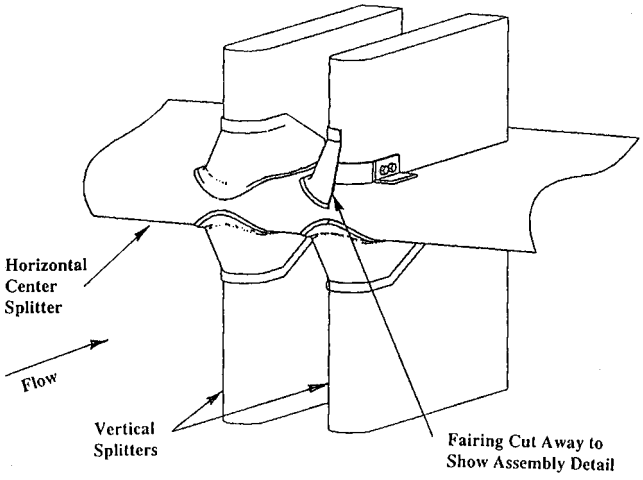

Fig. 19 Schematic of the silencer vanes and the fairing for reducing noise generated by the bolt heads.

In an earlier section, it was stated that there are numerous sources of noise and that acoustic data might easily be corrupted. We illustrate this possibility with the following example. Apart from reducing the internally generated noise by the rig, our efforts concentrated on reducing the background noise in the chamber as well. It had been established that the noise of the tunnel flow over acoustic tiles, on the silencer vanes in the exhaust collector of the wind tunnel, was a major source of noise. To mitigate this problem, the existing acoustic tiles were replaced with fine-mesh screens, which had generated much lower self-noise in bench tests. However, when the installation was complete, it was noticed that the tunnel background noise was actually higher at all angles. Further investigation revealed that the tunnel flow over the bolt heads, used to fasten the screens to the silencer vanes, was generating midfrequency noise. A fairing was designed and installed to overcome this problem, as shown in the schematic in Fig. 19. Figure 20 shows the background noise spectra, with and without this fairing, at three angles, 50, 90, and 145 deg. Surprisingly, the noise generated by the flow over the bolt heads was quite strong, ~5 dB over the tunnel noise and propagated to even the most forward microphone 50 ft away. This example demonstrates clearly that one has to exercise utmost caution in taking acoustic data.

3. *Quantitative Comparisons*

Thus far, we have concentrated on spectral shape and qualitative goodness of the measured spectra. However, spectral levels are very important. To make quantitative comparisons, a set of high-quality data must be available. At Boeing, such data were acquired in the 1970s and 1980s using a different rig, called the Quiet Dual Flow Rig (QDFR). A brief description of this rig is now provided. The QDFR was designed specifically to eliminate/minimize upstream noise so that pure jet noise could be measured. Both the primary and secondary 10-in. air supply lines emptied into propane burner cans of 15-in. diameter. The pipes downstream of the burner were 24 in. in diameter, with the inside of each lined with 2-in. ceramic fiber insulation and a stainless-steel facesheet. Each stream then passed through a 6-ft-diam muffler section 26 ft long and emptied into a larger plenum. Finally, the flow entered the nozzle, after passing through a flow straightener/screen section. The large plenum tanks were filled with heated air at required temperatures, and the rig was operated in a blowdown mode when acoustic data were acquired. The rig was massive and weighed over 100 tons. The carefully designed rig ensured that the combustor and all upstream noise were eliminated and that the upstream flow velocities were low. This rig had immense flow capability; in fact, in one application the rig was used as a 4-ft free wind tunnel for a fan noise test. The QDFR represented the best possible design for a jet rig and was used extensively for early jet noise research at Boeing, notably by Lu.[7,8] However, this rig was decommissioned in the late 1980s, for several reasons. First, its massive size precluded the incorporation of a wind tunnel in the anechoic chamber; second, data acquisition was time consuming because of the need to fill a large plenum with heated air and for the system to attain thermal equilibrium.

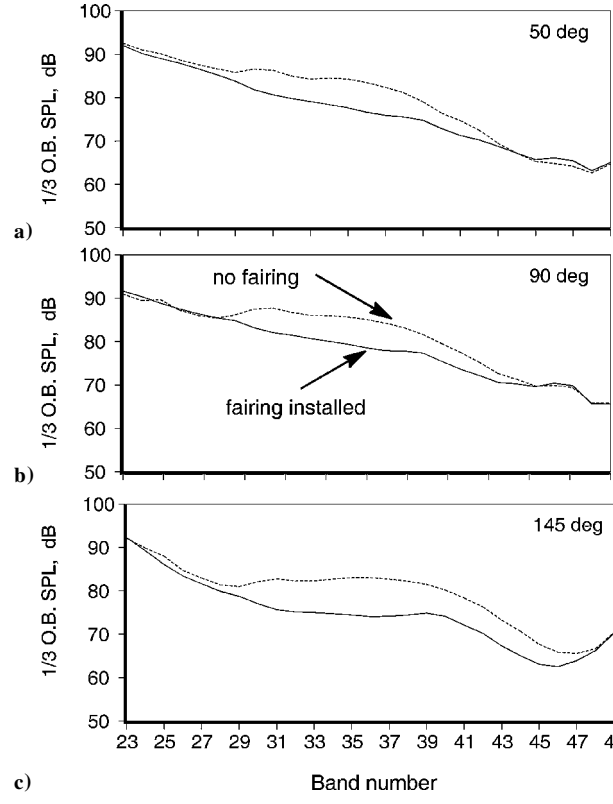

Fig. 20 Increase in background noise due to tunnel flow over bolt heads and its elimination, $M_t = 0.32$.

The author's goal from the outset was to try to reproduce the same spectra with the NTL3800 rig as was acquired with the QDFR. It was well recognized that the attainment of this objective presented a daunting challenge, given the constraints. One of the first issues to consider was the tremendous advances in the data acquisition system in the past 20 years and to ensure that there were no inherent differences caused by the different measurement systems. In the earlier tests, one-third-octave analyzers with analog filters were used to process the time signal and produce one-third-octave spectra. Recently, Boeing upgraded the data system, with Hewlett–Packard Co. E1433B analyzers. This system provides the capability for the acquisition of narrowband data of desired bin spacing and frequency range and simultaneous data acquisition from 40 channels. In the current tests, very fine narrowband data with a bin spacing of 23.4 Hz were acquired and synthesized to produce one-third-octave spectra, up to a center band frequency of 80,000 Hz. To verify that the one-third and narrowband analyzers yielded the same one-third-octave spectra for a given time signal, the output from one of the microphones was fed into the two different analyzers. Comparisons of one-third spectra obtained from the one-third analyzer and synthesized spectra from the narrowband analyzer are shown in Fig. 21. The spectra at three Mach numbers of 0.8, 0.9, and 1.0 from unheated jets and at an angle of 130 deg are shown. The two sets of data are virtually identical, except for minor differences at very low frequencies. This is not surprising given that the frequency range for the lowest one-third centerband frequencies is quite narrow, thereby introducing some error.

Having established that direct comparisons between the old and new data are meaningful, we now proceed to quantitative comparisons. Even though significant progress was made in reducing rig noise during the earlier effort, as demonstrated in Figs. 14 and 15, it was realized that further improvements were necessary.

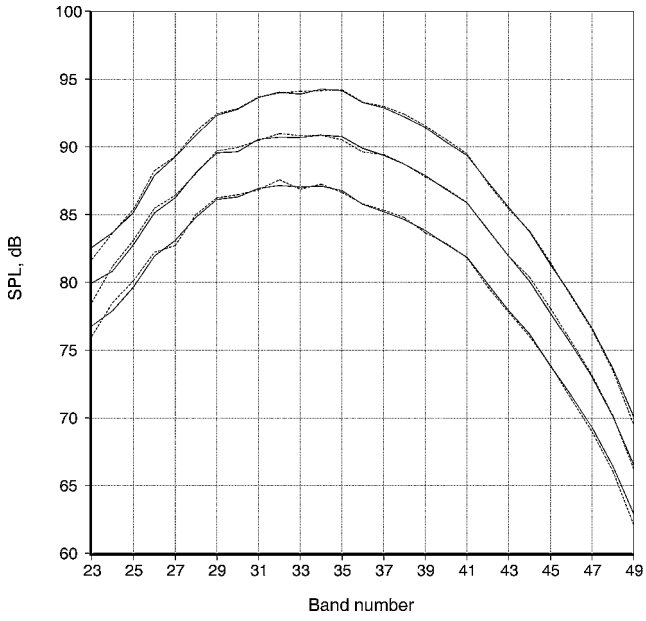

Fig. 21 Comparison of measured one-third-octave spectra with synthesized narrowband spectra; angle = 130 deg, M_j = 0.8, 0.9, and 1.0: ——, measured and - - - -, synthesized.

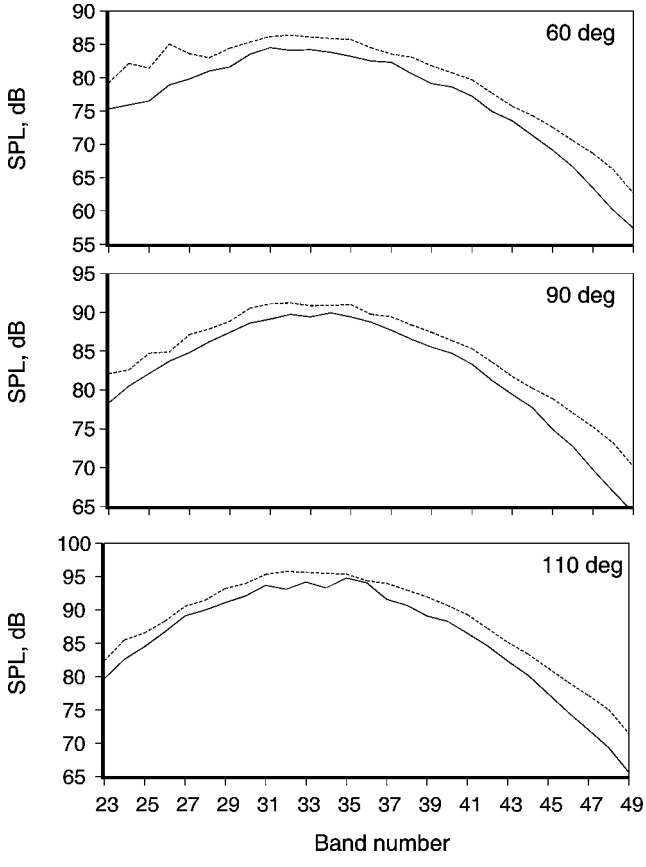

Fig. 22 Comparison of NTL3800 spectra with QDFR spectra, coaxial nozzle, A_s/A_p = 3.0, NPR_p = 1.55, T_p = 1456°R, NPR_s = 1.4, and T_s = 540°R: ——, QDFR and - - - -, NTL3800.

Examination of the spectra in Fig. 15 reveals the presence of jaggedness and some humps. In the second round of rig improvements, data were first acquired with the same nozzles used in the QDFR tests to assess the magnitude of the rig noise problem. Sample results are shown in Figs. 22 and 23 from a coaxial nozzle of area ratio 3.0, at two cycle conditions. As can be seen, the NTL3800 data have a higher spectral level at all frequencies. The magnitude of the discrepancy varies from 3 to 5^+ dB depending on the frequency,

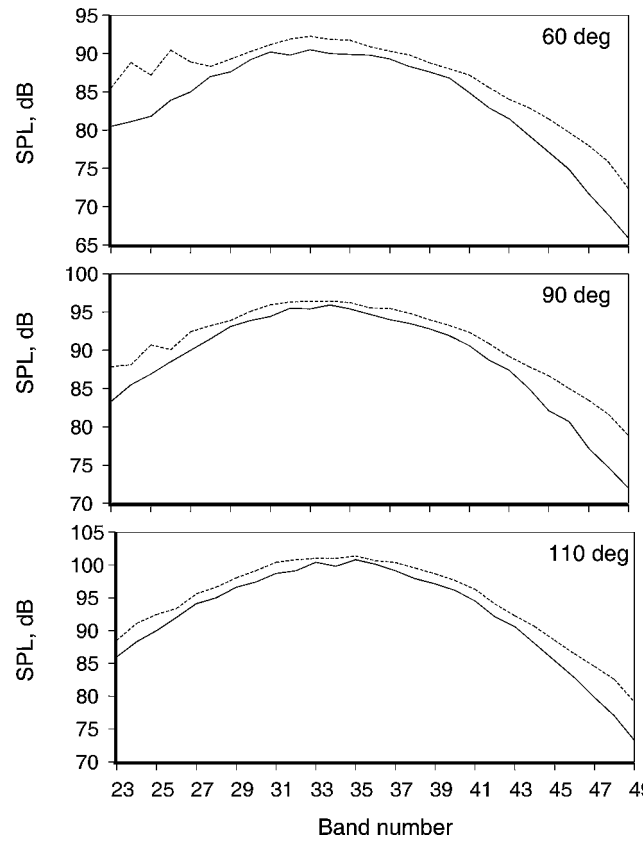

Fig. 23 Comparison of NTL3800 spectra with QDFR spectra, coaxial, nozzle, A_s/A_p = 3.0, NPR_p = 1.88, T_p = 1455°R, NPR_s = 1.8, and T_s = 540°R: ——, QDFR and - - - -, NTL3800.

radiation angle, and nozzle conditions. There are some tones at the lowest frequencies, especially at the most forward angles, the magnitude of which increase with the NPR of the primary stream. It is important to note another fact. The spectral shapes of the NTL3800 data more or less conform to that of the universal shape, even though the levels are off. It should be clearly recognized that the goodness of the spectral shape alone does not guarantee good data. Additional modifications to the rig were implemented, to further eliminate rig noise and to address the problem of elevated spectral levels. Several upstream treatments were attempted till satisfactory results were obtained.

Results of the recent round of modifications are now presented. Figures 24–26 show spectral comparisons between QDFR data and recent measurements, again from a coaxial nozzle of area ratio three. Figures 24–26 each show comparisons spanning a wide range of radiation angles. The jet operating conditions range from low power to very high subsonic Mach numbers and represent commercial engine cycles. Let us examine Figs. 24–26 in detail. In Fig. 24, for the lowest power shown, there is excellent agreement between the two sets of data, except for the tones at 250 and 400 Hz, at the lower emission angles. Figure 25, which is at the power setting as in Fig. 22, shows the dramatic reduction in the spectral level achieved and a good match with QDFR data. The agreement is excellent at 90 deg which indicates a reduction of 3–6 dB across the spectrum (Fig. 22). In Fig. 26, we see a similar improvement and good agreement with the QDFR data for the highest power. Figure 26 corresponds to the comparison shown in Fig. 23. For all of these cases, the two sets of data are identical at large angles where there is peak noise radiation. Any discrepancy shows up at low angles, with the spectra at 60 deg purposely chosen to illustrate another problem. In addition to the slightly elevated levels at the higher frequencies in Fig. 26, the presence of tones at the lower frequencies is obvious in Figs. 24–26. As we go aft, the impact of the tones becomes less pronounced. This is not to imply that the tones do not radiate to aft angles. Rather, the increase in jet noise with angle masks the tones, providing smooth

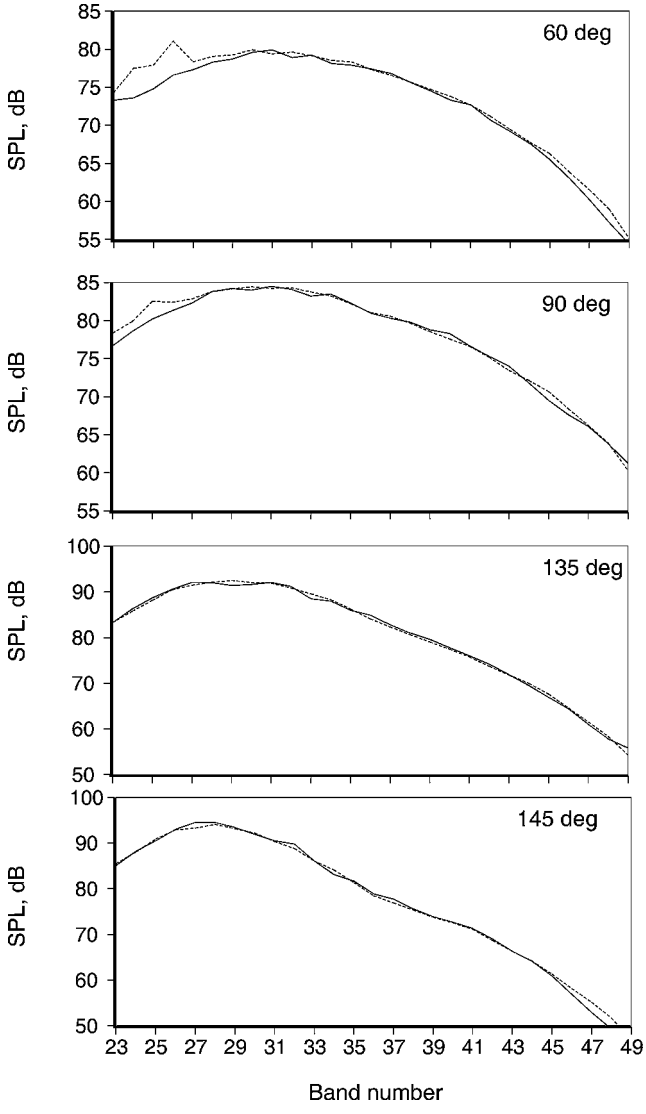

Fig. 24 Comparison of NTL3800 spectra with QDFR spectra, coaxial nozzle, $A_s/A_p = 3.0$, $NPR_p = 1.24$, $T_p = 1394°R$, $NPR_s = 1.34$, $T_s = 600°R$: ——, QDFR and - - - -, NTL3800 after rig improvements.

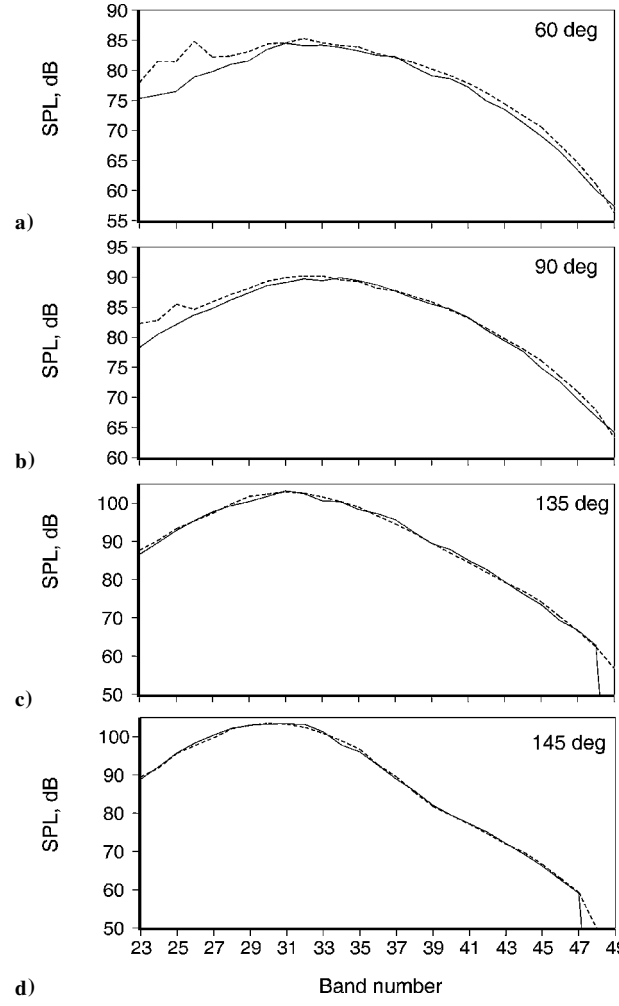

Fig. 25 Comparisons after rig improvements; same conditions as in Fig. 22.

spectra at large angles. A very detailed study of these tones has been carried out for a single jet by means of in-duct measurements with Kulite pressure transducers at two locations in the primary supply pipe. Many characteristics of these tones such as their amplitudes, absolute and relative to the adjacent broadband noise, and variations due to NPR, mass flow, effect of heating, etc., have been established. However, it is not clear as to what can be done about these tones. The need to measure thrust and noise simultaneously places several constraints on the overall design of the rig. There are several bellows and isolators in the supply pipes to absorb and transmit the loads in the three directions. For their intended function, the bellows must be flexible, and stainless-steel inserts inside the bellows cannot be fixed rigidly at both ends. Any low-frequency tones in the upstream supply pipes could excite these bellows, which cannot be damped. The amplified tones then enter the combustor, where they amplify the combustor noise and vice versa. The upshot of the arrangement is that these tones propagate to the far-field microphones. However, note a very important observation: These tones do not seem to lead to broadband amplification of jet noise in the far field. Examination of the spectra in Figs. 24–26 indicates clearly that, even though these tones are present in the recent data, there is excellent agreement at higher frequencies with the QDFR spectra, which do not have these tones. This fact permitted the author to defer this problem to a later date. Because of space constraints, the exact modifications that produced the rig noise reduction are not described. However, it is important to ensure that the nozzle performance does not get altered during the incorporation of noise fixes. We illustrate this point in Fig. 27, where the variation in nozzle discharge coefficient with NPR is shown, for four different upstream treatments. The coefficients follow the same consistent trend and are highly repeatable.

The preceding results demonstrate the tremendous advances made in enhancing the quality of data. One only has to compare the spectra in Fig. 14 with those in Figs. 24–26 to appreciate the magnitude of the improvement. This achievement is all the more commendable given the size of the current rig relative to that of the QDFR. The conflicting requirement for the simultaneous measurement of nozzle performance along with noise necessarily introduces complications and places additional constraints on rig design. However, it has been illustrated clearly that the quality of the acoustic data is comparable to that from the massive QDFR, except for the low-frequency tones at low radiation angles. Note that the QDFR was designed specifically to eliminate rig internal noise and had no capability to measure thrust.

IV. Issues with Nozzle Size

We now address issues associated with testing nozzles of different sizes using a given jet rig. It was stated in a preceding section that the size of the rig is dictated by considerations of size of the wind tunnel, wind-tunnel blockage effects, etc. The size of the NTL3800 jet rig was chosen such that it was compact and provided certain flow requirements, as described in Sec. I. What size nozzle should then be used in acoustic tests? Let us first review the

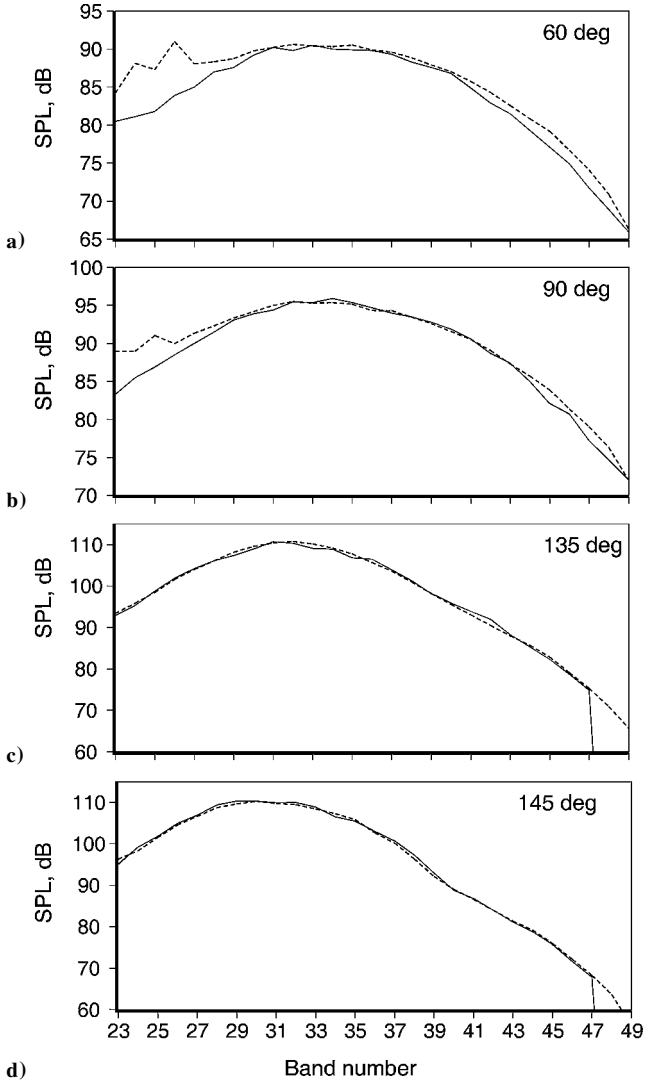

Fig. 26 Comparisons after rig improvements; same conditions as in Fig. 23.

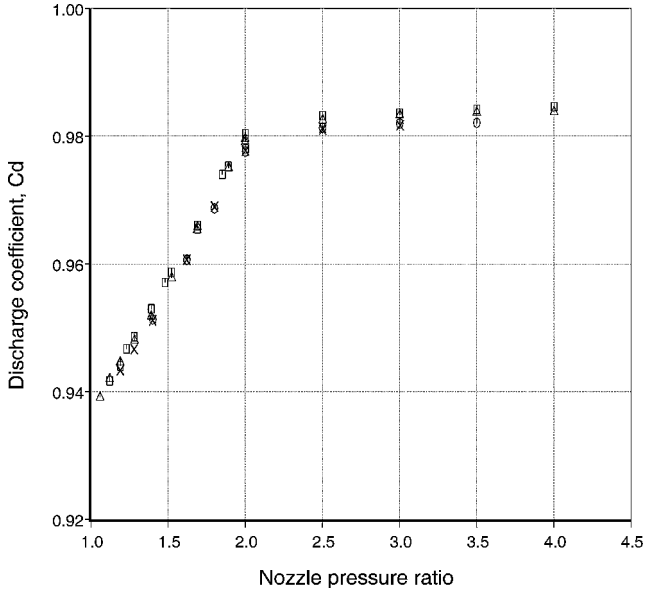

Fig. 27 Variation of nozzle discharge coefficient with NPR: symbols, different upstream rig modifications.

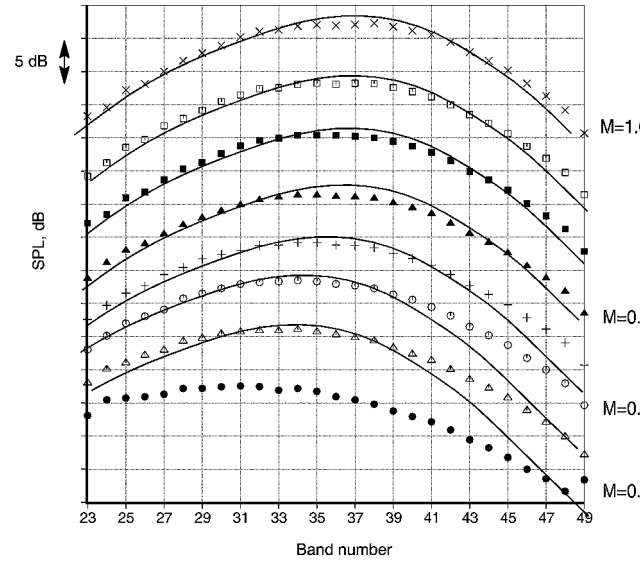

Fig. 28 Comparison of spectra at 90 deg from cold jets, d = 2.45 in.: ●, M = 0.3; △, M = 0.4; ○, M = 0.5; +, M = 0.6; ▲, M = 0.7; ■, M= 0.8; □, M = 0.9; ×, M = 1.0; and ——, FSS spectrum.

requirements of a model test. For industry applications, especially for the simulation of full-scale engines, the scaled frequencies from the model test should cover the frequency range of interest for the engine. For airplane certification this frequency range is from 50 to 10,000 Hz. Now, one can measure acoustic data accurately up to a one-third-octave centerband frequency of 80,000 Hz. Obviously, an eighth-scale nozzle is desirable and would provide the requisite information. When smaller nozzles are tested, one is forced to extrapolate or create data at the higher full-scale frequencies in the computation of noise metrics. This practice might be acceptable for simple nozzles, the spectral characteristics from these being well established. However, when complex nozzles with exotic shapes need to be developed for noise suppression, this practice breaks down and an eighth-scale model becomes necessary for data fidelity.

We now examine the consequences of testing nozzles of different diameters on data quality. Again we use concrete examples to elucidate the main effects. Spectra from unheated jets at a range of Mach numbers were presented in Fig. 12 from a nozzle of diameter 1.5 in. We show similar spectra at 90 deg from a larger nozzle of 2.45-in. diameter in Fig. 28, along with the similarity spectrum at each Mach number. For this nozzle, there is excellent agreement for Mach numbers of 0.7 and higher. The rig noise becomes a factor at the higher frequencies for the $M = 0.6$ jet. For the lower Mach numbers of 0.4 and 0.5, the spectral levels above a frequency of 20,000 Hz are significantly off, of the order of 5 or more dB. Let us take this exercise a step further, with a much larger nozzle of diameter 4.45 in. and examine the spectra in Fig. 29. Even at the higher Mach numbers, the spectral shapes do not conform to that of the similarity spectrum. As we increase the size of the nozzle, the mass flow increases for a fixed Mach number. This higher mass flow through the system results in higher internal velocity in the supply pipes and, hence, higher internally generated noise. Even though the larger nozzle generates more pure jet noise, the strength of the internal noise, which depends on a high exponent of velocity, increases at a much faster rate. Furthermore, the smaller nozzle has a lower transmission of internally generated noise. This is why the spectra begin to get corrupted at higher Mach numbers for larger nozzles, as seen in Figs. 12, 28, and 29. We purposely chose unheated jets to illustrate this point because the jet noise levels are low for unheated jets and the mass flows are the highest for a given Mach number. In the preceding examples, the contraction ratio for the largest nozzle is ~3, and the internal velocities are consequently very high. Evidently, one should not attempt to measure noise at low

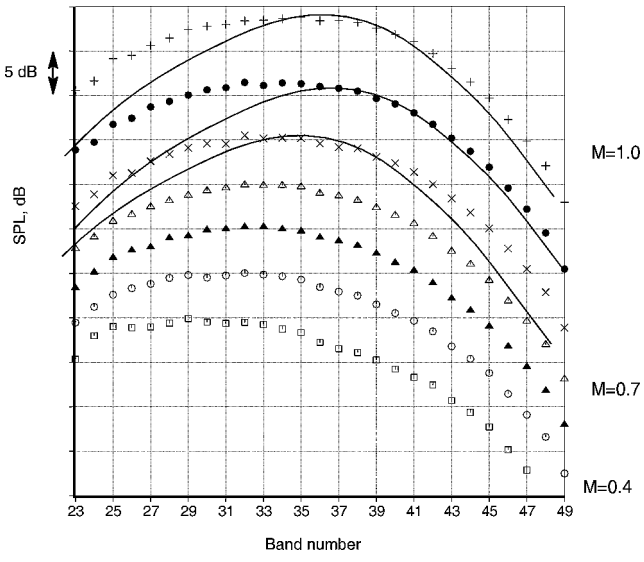

Fig. 29 Comparison of spectra at 90 deg from cold jets, d = 4.45 in.: □, M = 0.4; ◌, M = 0.5; ▲, M = 0.6; △, M = 0.7; ×, M = 0.8; ●, M = 0.9; +, M = 1.0; and ——, FSS spectrum.

subsonic Mach numbers with very large nozzles, without taking extraordinary measures to control upstream noise. It is important to understand the test requirements, the cycle points, rig constraints, etc., in choosing the proper size of the nozzle to avoid measuring contaminated data. One cannot make a general statement about the quality of noise data from a particular test setup without specifying the nozzle size and the jet reservoir conditions. The requirement for a compact rig indeed imposes restrictions that must be comprehended and heeded.

Before we move on, we show one final quantitative comparison with QDFR data, from a conic nozzle of 3.46-in. diameter. The jet Mach number is 1.37 and temperature ratio is 2.8 in Fig. 30. There is excellent agreement between the two sets of data, except for the low-frequency noise (at low angles) in the current data. Surprisingly, even the screech tones line up exactly at the same frequencies and have the same amplitude although the upstream geometries are different. Agreement at other nozzle conditions (not shown here) was equally good. The supersonic case was chosen to highlight another feature. Recall that the current one-third-octave data in Fig. 30 were synthesized from narrowband data. It is clear that this process is valid even for data that contain shock-associated noise and screech tones. This example provides additional validation for the current process (also Fig. 21).

V. Implications

The importance of data quality and the critical role that data play in the development of theories for predicting jet noise and in the development of technology for noise suppression are obvious, as discussed in Sec. I. As part of a broad effort to evaluate the status of jet noise technology, the author carried out an extensive analysis of available jet noise data from various facilities, with special emphasis on noise suppression. The major findings of this study are summarized here. Most data suffer from contamination from nonjet sources and the spectra are of poor quality, as shown in Figs. 31–33 from three different facilities/rigs. Figure 31 shows measured spectra at 90 deg from heated jets at high subsonic Mach numbers. The spectral shapes clearly indicate that the rig noise has corrupted the data. Contrast the spectral shapes with those in Figure 12 to recognize the problems with this set of data. In Fig. 32, we show spectra from a different facility at two radiation angles, for a range of Mach numbers. Note the anomalous trends at the higher frequencies, with a well-pronounced hump above 30,000 Hz. Figure 33 shows spectra from a third rig, obtained with a coaxial nozzle at typical engine conditions. A more insidious situation prevails with these types of spectra. Whereas the problems are obvious with the data shown

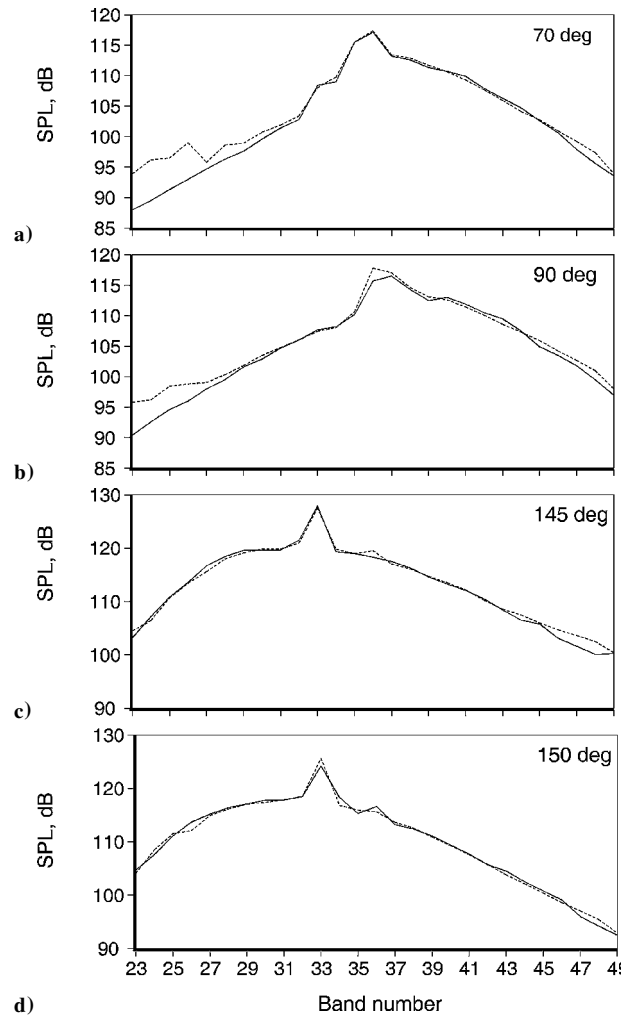

Fig. 30 Comparison of NTL3800 spectra with QDFR spectra, d = 3.46 in., NPR = 3.0, and T_r/T_a = 2.8: ——, QDFR and - - - -, NTL3800.

in Figs. 31 and 32, the spectra shown in Fig. 33 are smooth and appear to be all right at first look. Only a deeper analysis reveals that the high-frequency data start deviating at 10,000 Hz and the discrepancy keeps increasing with frequency. The magnitude of the contamination is over 12 dB at the higher frequencies, rendering the data useless.

One cannot dismiss the problems at high frequency in a cavalier fashion for the following reasons. It is not adequate to obtain good measurements at the peak frequency with small nozzles. When extrapolated to full scale, the spectra at the higher frequencies from the model scale lie precisely in the range of frequencies for which the annoyance penalty is maximum in the evaluation of the noise metrics. Therefore, it is of vital importance to measure pure jet noise at all frequencies and at all angles. Another issue pertains to the phenomenon of broadband amplification of jet noise due to upstream excitation. The spectra shown in Figs. 31–33 were obtained at static conditions in well-established anechoic chambers. Therefore, it is clear that there is a high level of rig internal noise, possibly amplifying jet noise and vice versa. The spectra measured at the far-field microphones are a combination of the jet noise, rig noise, and possible interaction of the two sources in unknown fashion. Note that nothing has been mentioned about the amplitudes in the preceding examples. Lu,[7] for example, clearly demonstrated the magnitude of broadband amplification due to artificial excitation, from a pure tone as well as from a broadband excitation source. His measurements were obtained with the QDFR, which has very little upstream noise. Therefore, it is entirely conceivable that the more recent tests at many facilities were conducted unwittingly in an excited mode. Furthermore, the conflicting reports on the effect

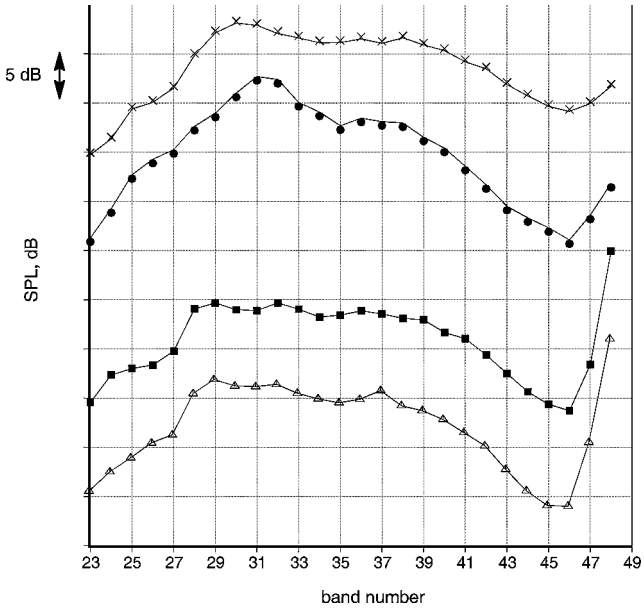

Fig. 31 Typical spectra from facility 1; round nozzle, heated, high subsonic jet, and angle = 90 deg.

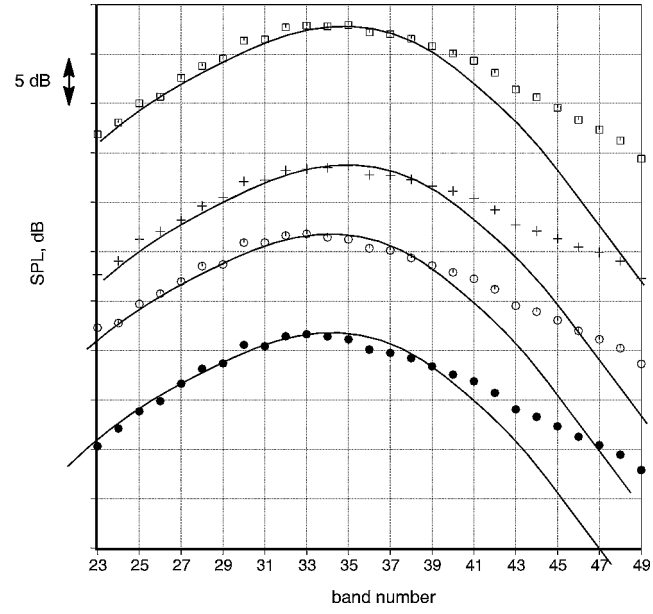

Fig. 33 Typical spectra from facility 3; coaxial nozzle, typical engine conditions at takeoff power.

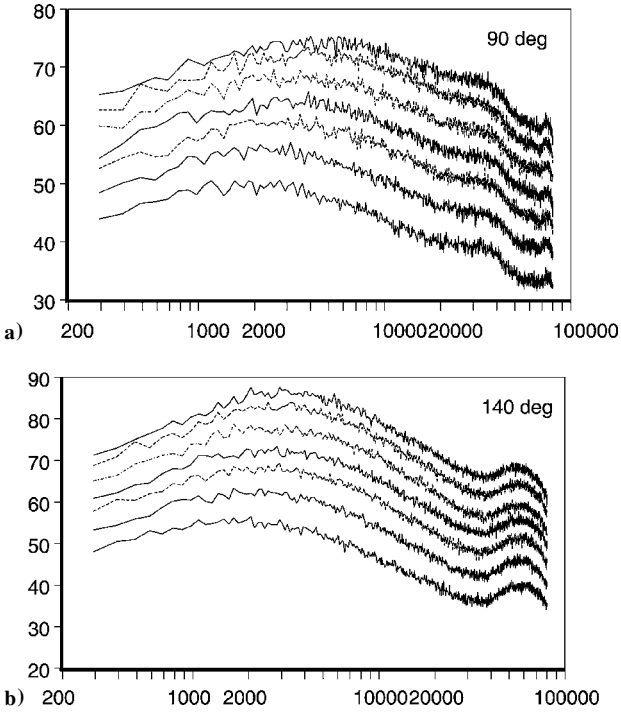

Fig. 32 Typical spectra from facility 2; round nozzle, cold jets, M = 0.4, 0.5, 0.6, 0.7, 0.8, 0.9, and 1.0.

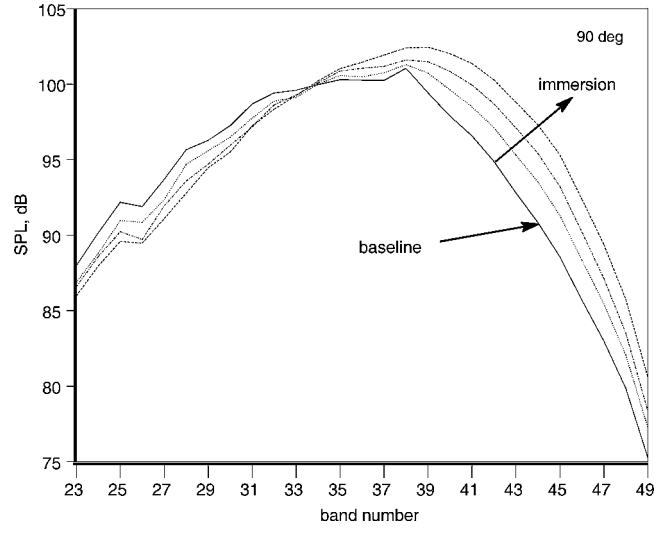

Fig. 34 Effect of chevron immersion on radiated noise, angle = 90 deg: ——, baseline; · · ·, low immersion; –·–·, medium immersion; and - - - -, high immersion.

of a given excitation may well be due to the level of the rig internal noise, masking the true role of the strength of the excitation source.

Finally, we turn our attention to a currently popular noise reduction device, the chevron. Chevrons have been studied extensively in the past few years, and major noise reductions have been quoted; for example, see Saiyed et al.[9] In Fig. 34 we show the effects of incorporating three different chevrons on the measured spectra, at typical takeoff power and at 90 deg. These data, obtained after the completion of the rig improvements, indicate that the chevrons do reduce the low-frequency noise level, but lead to a tremendous amount of noise increase at the higher frequencies. The three chevrons had different amounts of immersion into the flow. It has been found that increasing the immersion yields more reduction of low-frequency noise. However, there is a corresponding greater increase in the high-frequency noise. Let us suppose that we carry out the same test with one of the other rigs, with significant rig noise. If the noise contamination happens to be at the higher frequencies, the increase in high-frequency noise from the nozzle with chevrons will be masked by the rig noise. One might observe the noise reduction at the lower frequencies without uncovering the tremendous increase in high-frequency noise. When calculating the noise metric such as the flyover EPNL, one could easily overestimate the noise benefit because of neglecting the increase in noise at the higher frequencies, while taking credit for noise reduction at the lower frequencies. Also, the ranking of the different chevrons in terms of their efficacy in reducing noise would be in error, potentially leading to the selection of the wrong chevron for actual application. Note that the effect on EPNL is to a large extent dependent on the engine cycle, engine scale, the interplay between the low-frequency reduction and high-frequency increase, noise directivity, etc. There is another, more disturbing

aspect as well. Flowfield surveys as well as computational fluid dynamics, for example see Figs. 17–20 in Ref. 10, have shown that the flowfields are vastly different for the baseline and chevron nozzles. The chevrons tend to split the main jet into several minijets, with a highly convoluted shear layer. The shear layer is uniform for the baseline nozzle, whereas it is complex for the chevron nozzle. One cannot know with certainty whether the reported reduction in far field noise is actually due to the chevrons or caused by the different paths encountered by the rig noise as it propagates to the far field.

It is clear from the preceding discussion that the quoted benefits in noise reduction due to modifications to the nozzle trailing edge need to be carefully evaluated. Typically, the reduction in low frequency is ~3 dB. However, the magnitude of the contamination is much higher in the recent data. Sometimes it is claimed that even though the absolute measurements for the baseline and chevron nozzles are in error, the observed noise reduction is a valid quantity. Again, there is no basis for such a claim because the spectral shapes are modified by the chevrons (Fig. 34) and because of reasons discussed in the foregoing paragraph. In no way is it suggested here that these devices are without merit; rather, it is emphasized that extreme care must be exercised in the evaluation of these devices and in the interpretation of the data.

VI. Summary

The results of a major undertaking in acquiring aeroacoustic data of high quality have been reported. Descriptions of a jet simulator, incorporated with a six-component force balance have been provided. Many problems associated with initial data from this rig and suitable modifications to eliminate these problems have been described. Significant improvements in the quality of flow and acoustics have been demonstrated. The level of distortion in both pressure and temperature has been minimized to provide a nearly uniform flow at the nozzle entrance section. This uniform flow provides the ability to set desired nozzle conditions accurately. The capability of the force balance has been evaluated by comparing the measured aerodynamic performance of a cubic nozzle with measurements obtained using a well-established balance at the Boeing NTF. Excellent agreement over the entire range of NPR has been demonstrated.

The biggest advances were made in improved acoustic data quality. It was shown with detailed examples that rig internal noise is a big concern and that extreme care is required for the acquisition of good data. Qualitative evaluations may easily be carried out through comparisons with the fine-scale similarity spectrum of Tam et al.[5] Apart from the significance of the finding in itself, the observation in Ref. 5 has a valuable role in aiding experimenters, though they perhaps never intended it as such. It has been verified that the universal spectral shape at lower angles is maintained even when the jet is imbedded in an external stream. When the spectral shapes are smooth, as in Figs. 29 and 33, they appear to be in good order. This false sense of goodness in the past has prevented the identification of problems with data. A carefully designed blow-down rig that eliminates upstream noise represents the best possible simulator for jet acoustics. Quantitative comparisons with spectra from such a rig were provided for a wide range of nozzle conditions. Excellent spectral agreement was demonstrated from low subsonic Mach numbers to high subsonic Mach numbers from heated jets, at cycle conditions that represent those of typical commercial jet engines. The potential cause of some tones at very low model-scale frequencies ($\leq$400 Hz) and at lower radiation angles has been investigated. It was verified that these tones do not lead to broadband jet noise amplification.

It was illustrated with actual data that it is more difficult to measure pure jet noise from very large nozzles especially at low jet velocities, with a given compact rig. Extra measures are needed to control the higher internal noise for these applications. The objectives of an aeroacoustic test should be well understood and proper choice of nozzle configurations made to avoid acquiring data corrupted by extraneous noise. It is of paramount importance to measure clean noise at all angles and all frequencies for airplane applications because knowledge of the entire spectra is required to make proper engineering decisions.

A thorough analysis of available jet noise data from different facilities/rigs revealed that most spectra are contaminated by extraneous noise. Most practical prediction methodologies for jet noise are empirical in nature, for example, see Ref. 11. The Society of Automotive Engineers (SAE) methodology, developed in the mid-1980s, was based on the available database at that time. Since then, larger commercial jet engines with higher bypass ratios have been introduced. There is a need to extend the capabilities of the SAE method beyond the current range of parameters, to have predictive ability for such engines and to perform trade studies during the preliminary design of new aircraft. Therefore, it is vital to establish a database with high fidelity for these engine characteristics. The fidelity of data should be kept in mind when undertaking extensions of existing prediction methods. Development of noise suppression devices demands that extraneous noise not cloud the noise picture. Again, much of the measurements in this endeavor suffer from severe problems. It is clear then, that high-quality data is absolutely necessary to advance the state of jet noise technology.

VII. Conclusions

Issues that are important for jet aeroacoustic tests have been reviewed and discussed. It has been emphasized that test programs should address both the flow and noise issues. Simultaneous measurement of nozzle aerodynamic performance and noise is important, especially in the development of noise suppression devices. It has been demonstrated that the recent efforts at rig refurbishment have resulted in excellent data quality, in both aerodynamic performance and noise for a wide range of nozzle conditions. It is indeed remarkable that the quality of acoustics from a compact rig that also includes complexities due to thrust measurement is comparable to that of a massive blowdown rig. Note, though, that a monumental amount of work and improvements were necessary to achieve this high quality. The importance of understanding the limitations of a jet rig and the proper choice of nozzle size for achieving a given set of objectives in an aeroacoustic test is clearly established. An extensive analysis of acoustic data acquired in the past several years from various facilities indicated that most data are hopelessly contaminated. Theoretical approaches to jet noise prediction are very difficult as evidenced by the lack of a comprehensive theory after over 50 years of research. This difficulty should not be compounded by ambiguous experimental studies. It is obvious that a concerted effort from the experimental community is imperative to advance the field of jet noise prediction and suppression.

Acknowledgments

It is a pleasure to acknowledge the outstanding support provided by the Low Speed Aeroacoustic Facility test crew over the past several years. The author benefited greatly from the numerous discussions with H. Y. Lu, L. D. Arney, L. T. Clark, D. W. Boston, W. R. Miller, and M. C. Joshi of The Boeing Company. Special thanks are extended to Mahendra Joshi for offering many suggestions and editorial comments that improved this paper. The encouragement and insights provided by my esteemed colleagues in the High Speed Research/High Speed Civil Transport program from NASA Langley Research Center, NASA John H. Glenn Research Center at Lewis Field, and General Electric Aircraft Engines were very valuable.

References

[1]Fisher, M. J., Lush, P. A., and Harper Bourne, M., "Jet Noise," *Journal of Sound and Vibration*, Vol. 28, No. 3, 1973, pp. 563–585.

[2]Tanna, H. K., Dean, P. D., and Fisher, M. J., "The Influence of Temperature on Shock-Free Supersonic Jet Noise," *Journal of Sound and Vibration*, Vol. 39 No. 4, 1975, pp. 429–460.

[3]Tanna, H. K., "An Experimental Study of Jet Noise. Part I," *Journal of Sound and Vibration*, Vol. 50, 1977, pp. 405–428.

[4]Tanna, H. K., "An Experimental Study of Jet Noise. Part II," *Journal of Sound and Vibration*, Vol. 50, 1977, pp. 429–444.

[5]Tam, C. K. W., Golebiowski, M., and Seiner, J. M., "On the Two Components of Turbulent Mixing Noise from Supersonic Jets," AIAA Paper 96-1716, May 1996.

[6]Viswanathan, K., "Analysis of the Two Similarity Components of Turbulent Mixing Noise," *AIAA Journal*, Vol. 40, No. 9, 2002, pp. 1735–1744; also AIAA Paper 2001-2115, May 2001.

[7]Lu, H. Y., "Effect of Excitation on Coaxial Jet Noise," *AIAA Journal*, Vol. 21, No. 2, 1983, pp. 214–220.

[8]Lu, H. Y., "An Empirical Model for Prediction of Coaxial Jet Noise in Ambient Flow," AIAA Paper 86-1912, July 1986.

[9]Saiyed, N. H., Mikkelsen, K. L., and Bridges, J. E., "Acoustics and Thrust of Separate-Flow Exhaust Nozzles with Mixing Devices for High-Bypass-Ratio Engines," AIAA Paper 2000-1961, June 2000.

[10]Kenzakowski, D. C., Shipman, J., Dash, S. M., Bridges, J. E., and Saiyed, N. H., "Turbulence Model Study of Laboratory Jets with Mixing Enhancements for Noise Reduction," AIAA Paper 2000-0219, Jan. 2000.

[11]"Gas Turbine Jet Exhaust Noise Prediction," Society of Automotive Engineers, Paper SAE ARP876, Rev. D, Jan. 1994.

H. M. Atassi
Associate Editor